scientific reports

Check for updates

OPEN

HIV/AIDS compartmental model analysis with drug resistance treatment, vertical transmission, and optimal control theory

Olumuyiwa James Peter[1,2,3], Shewafera Wondimagegnhu Teklu[4]✉, Ghaniyyat Bolanle Balogun[5], Gbolahan Bolarin[6] & Manalebish Debalike Asfaw[7]

This study develops a novel HIV/AIDS compartmental model that integrates the critical, interconnected challenges of drug resistance emergence from treated individuals, healthcare constraints via a saturating treatment function, and persistent vertical transmission. The objective is to provide a comprehensive mathematical framework for analyzing these complex dynamics and designing effective intervention strategies. Our analysis reveals that treatment saturation can induce a backward bifurcation, complicating disease eradication efforts, while optimal control simulations demonstrate that a combined strategy of enhanced screening, accelerated treatment initiation, and adherence support significantly reduces infection pools and minimizes disease progression compared to isolated interventions.

Keywords HIV/AIDS model, Basic reproduction number, Stability analysis, Bifurcation analysis

The Human Immunodeficiency Virus/Acquired Immunodeficiency Syndrome (HIV/AIDS) remains one of the most significant global public health challenges of our time[1]. As of 2023, an estimated 39.0 million people were living with HIV globally, and despite progress, the epidemic was responsible for 1.3 million new infections and 630,000 deaths in the preceding year, underscoring its persistent threat[2]. The advent of antiretroviral therapy (ART) has been a pivotal turning point, transforming HIV from a terminal illness into a manageable chronic condition for many[3]. However, the long-term success of these programs is critically threatened by a complex interplay of biological and socio-economic factors, including persistent transmission routes, healthcare system constraints, and, crucially, the evolution of drug-resistant viral strains[4–6]. The emergence of drug-resistant HIV represents a formidable obstacle to the long-term success of antiretroviral therapy (ART) and global epidemic control. Resistance is an evolutionary process where the virus mutates under the selective pressure of medication, rendering drugs less effective. This process is critically accelerated by incomplete viral suppression, a common consequence of poor patient adherence to complex and lifelong treatment regimens[7]. On a clinical level, the development of resistance leads to virological failure, marked by a rebound in viral load, a decline in immune function, and an accelerated progression to AIDS, which necessitates a switch to more complex and often more toxic second- or third-line therapies[4]. The public health threat is magnified by the transmission of these resistant strains, which can severely compromise the efficacy of standard first-line treatments for newly infected individuals, thereby undermining national and global treatment guidelines[6]. The landscape of resistance is further complicated by the existence of numerous drug-resistant subtypes and the challenge of multidrug resistance, making clinical management increasingly difficult[5]. Consequently, mathematical models that explicitly incorporate the dynamics of drug resistance are essential tools for evaluating how factors like treatment coverage and healthcare resources influence its spread, and for designing sustainable public health strategies that can preserve the effectiveness of current and future therapies[8].

[1]Department of Mathematics, Saveetha School of Engineering, SIMATS, Saveetha University, Chennai, Tamil Nadu, India. [2]Department of Mathematical and Computer Sciences, University of Medical Sciences, Ondo City, Ondo State, Nigeria. [3]Department of Epidemiology and Biostatistics, School of Public Health, University of Medical Sciences, Ondo City, Ondo State, Nigeria. [4]Department of Mathematics, College of Natural and Computational Sciences, Debre Berhan University, Debre Berhan, Ethiopia. [5]Department of Computer Science, Faculty of Communication and Information Sciences, University of Ilorin, Ilorin, Nigeria. [6]Department of Industrial Mathematics, Federal University of Technology, Minna, Nigeria. [7]Department of Mathematics, Addis Ababa University, Addis Ababa, Ethiopia. ✉email: luelzedo2008@gmail.com; shewaferaw@dbu.edu.et

Mathematical modeling has become an indispensable tool for understanding the intricate transmission dynamics of infectious diseases like HIV/AIDS, with numerous recent studies demonstrating its utility in analyzing stability and simulating disease spread[9–11]. By translating complex biological and social processes into a system of mathematical equations, models allow researchers to dissect the key drivers of an epidemic, predict its future course, and evaluate the potential impact of various public health interventions, such as optimal control strategies[12–16]. This quantitative approach is crucial for designing evidence-based strategies that are both effective and resource-efficient. A primary challenge to the long-term control of HIV is the evolution of drug-resistant viral strains, a phenomenon often driven by poor patient adherence or incomplete viral suppression[7]. The emergence of resistance leads not only to individual treatment failure and disease progression but also to the potential for transmitting these compromised strains to others[4–6]. Therefore, understanding the dynamics of resistance emergence and its spread through the population is critical for developing robust models and sustaining the long-term effectiveness of ART programs.

Recent mathematical modeling efforts by Olaniyi and collaborators have significantly advanced the field of epidemiological dynamics across various diseases. Their work on HIV/AIDS has explored both autonomous systems with vertical transmission and nonlinear treatment[17] and, more recently, non-autonomous systems to investigate time-varying, cost-effective intervention strategies[18]. Beyond HIV, their methodological rigor has been applied to other pathogens, including a stability and intervention analysis of Rift Valley fever[19] and a Lyapunov stability and economic evaluation of monkeypox dynamics incorporating vertical transmission[20]. This group has also demonstrated expertise in modeling complex public health issues beyond infectious diseases, such as substance abuse with real data integration[21]. A common strength of these studies is their focus on rigorous stability analysis and the evaluation of optimal control measures. However, a review of this body of work reveals a specific gap relevant to the long-term management of HIV: while the models in[17,18] effectively address treatment and interventions, they do not explicitly incorporate the critical phenomenon of drug resistance emerging from the treated population. This omission is significant, as drug resistance is a primary obstacle to the sustainability of antiretroviral therapy (ART) programs. To address this gap, our study develops a novel deterministic compartmental model that uniquely integrates the interconnected dynamics of (i) a saturating treatment function reflecting healthcare constraints, (ii) the emergence of drug resistance from the treated compartment, and (iii) persistent vertical transmission. The novelty of our work lies in this unified framework, which allows for a detailed investigation of how treatment saturation can induce a backward bifurcation a complex behavior with profound implications for disease eradication and facilitates the design of an optimal control strategy that specifically targets the suppression of drug-resistant strains, a challenge not simultaneously tackled in the aforementioned studies. Other mathematical models have been instrumental in exploring HIV dynamics, with studies focusing on local and global stability analysis and the simulation of parameter impacts on disease spread[7,9,10]. A key feature in many models is the inclusion of vertical transmission; despite successful prevention of mother-to-child transmission (PMTCT) programs, an estimated 130,000 new infections occurred in children in 2022, highlighting it as a persistent driver of the epidemic across generations[2,22]. Another critical real-world factor is the capacity of healthcare systems. As of 2022, approximately 29.8 million of the 39.0 million people living with HIV were on ART, a gap that justifies using a nonlinear, saturating treatment function to model bottlenecks in care that can influence the dynamics of drug resistance[2,8]. The evolution of drug-resistant strains, driven by factors like incomplete viral suppression, is a central challenge, as maintaining the required **>95%** adherence level is difficult for many patients[4–6]. To address these multifaceted challenges, Optimal Control Theory (OCT) offers a powerful framework for designing dynamic intervention strategies to minimize infections and mortality[12,13,23]. Furthermore, bifurcation analysis has been a pivotal tool for uncovering complex behaviors, such as the backward bifurcation phenomenon, which has profound public health implications as it suggests that simply bringing the basic reproduction number below unity may not be sufficient to eradicate the disease[24].

The landscape of the HIV/AIDS modeling has expanded considerably to capture increasing epidemiological complexities, including co-infections with diseases like pneumonia, COVID-19, and Hepatitis[23,25–34] and demographic structures such as age[35]. Furthermore, critical individual factors like drug resistance[5,7], healthcare constraints via saturating treatment functions[8], and vertical transmission[22] have been studied. However, a significant gap persists, as these critical dynamics are often explored in isolation. A comprehensive framework that simultaneously integrates the deeply synergistic interplay of drug resistance emergence, treatment saturation, and vertical transmission remains underdeveloped. This is a crucial omission, as these factors are interconnected: treatment saturation can exacerbate selection pressure for drug resistance, while vertical transmission perpetuates the epidemic by creating a continuous pool of individuals who will eventually strain the treatment system.

To address this gap, we propose a novel deterministic compartmental model whose novelty lies in its unified framework that concurrently incorporates the emergence of drug resistance from the treated population, a nonlinear saturating treatment function reflecting healthcare constraints, persistent vertical transmission, and the mitigating effect of media awareness. The primary objectives of this study are twofold: first, to conduct a rigorous qualitative analysis of this comprehensive model, including deriving the basic reproduction number, analyzing equilibrium stability, and investigating bifurcation phenomena; and second, to apply optimal control theory to design a dynamic, multi-pronged intervention strategy. By analyzing how the combined factors induce complex behaviors like backward bifurcation and formulating optimal control strategies to mitigate them, this work provides a significant extension to the literature and a more realistic tool for public health planning.

The remainder of this paper is organized as follows: Sect. “Model formulation” details the formulation of the mathematical model. Section “Theoretical analysis” presents the qualitative analysis of the model, including its fundamental properties, equilibrium points, and bifurcation analysis. Section “Sensitivity analysis” is dedicated to the sensitivity analysis, where we identify the parameters that most significantly influence disease transmission. Section "Optimal control problem and analysis" formulates the optimal control problem and

derives its solution. Section "Numerical simulation results and discussions" provides numerical simulations to illustrate our analytical findings and demonstrate the effectiveness of the optimal control strategies. Finally, Sect. "Conclusions and Future Directions of the Study" offers conclusions and discusses potential directions for future research.

Model formulation

To better understand and control the transmission dynamics of HIV/AIDS, we propose a deterministic compartmental model that integrates key epidemiological and social factors: the development of drug resistance, healthcare system constraints, media-driven awareness, and comprehensive vertical transmission. The total human population, $N(t)$, at any time t is divided into six mutually exclusive compartments: susceptible individuals ($S(t)$), unaware HIV-infected individuals ($I_a(t)$), aware HIV-infected individuals not yet on treatment ($I_b(t)$), individuals on ART for drug-sensitive HIV ($T(t)$), individuals infected with drug-resistant HIV ($R(t)$), and individuals who have progressed to full-blown AIDS ($A(t)$) such that the total human population is represented by:

$$N(t) = S(t) + I_a(t) + I_b(t) + T(t) + R(t) + A(t). \tag{1}$$

The population is sustained by a constant birth rate, κ. However, the inflow into the susceptible class is reduced by vertical transmission, a fraction q of infants born to mothers from any of the infected compartments (I_a, I_b, T, R, or A) become infected at birth. Consequently, only the remaining fraction of newborns enter the susceptible class. Susceptible individuals become infected through contact with infectious individuals. This transmission process is modulated by a constant media awareness parameter, m, where $0 \leq m < 1$, which reflects the impact of public health campaigns and general awareness in reducing high-risk behaviors, thereby lowering the effective transmission rate. The relative infectiousness of different groups is accounted for by modification factors τ_1, τ_2, τ_3, and τ_4. These factors are all assumed to be less than one, reflecting a reduction in transmission compared to the baseline infectiousness of the unaware group (I_a). Specifically, we assume a hierarchy of infectiousness such that $1 > \tau_1 > \tau_2 > \tau_3 > \tau_4$. This hierarchy represents the combined effects of awareness and disease progression: aware individuals (τ_1) are assumed to adopt safer behaviors; treated individuals (τ_2) benefit from suppressed viral loads; and individuals with resistant HIV (τ_3) or advanced AIDS (τ_4) are assumed to have a lower overall contribution to new infections, potentially due to reduced activity levels associated with illness, despite their high viral loads. Upon infection, susceptible individuals move into the $I_a(t)$ class, which consists of HIV-infected individuals who are unaware of their status. These individuals are a key driver of the epidemic due to potentially higher-risk behaviors. They may be identified through screening at a rate α, transitioning them into the $I_b(t)$ class. Individuals in $I_b(t)$ are aware of their HIV-positive status but have not yet started treatment. Crucially, this compartment is also populated by newborns infected through vertical transmission. A fraction q of infants born to mothers from any infected compartment enter this aware class directly, reflecting immediate diagnosis at birth as part of modern PMTCT (Prevention of Mother-To-Child Transmission) protocols. Unaware individuals who are not detected in time may progress directly to AIDS at rate σ. Individuals in $I_b(t)$, who are aware of their infection, may begin ART at a nonlinear rate $\frac{\theta I_b}{1+\rho I_b}$. The denominator term, $1 + \rho I_b$, captures the phenomenon of treatment saturation, where healthcare system capacity limitations can slow the rate of ART initiation as the number of eligible individuals grows. Those who do not receive treatment in time may progress to AIDS at a rate ξ. Treated individuals move into the $T(t)$ class. Over time, due to factors like poor adherence or incomplete viral suppression, a fraction of these individuals may develop drug resistance, transitioning to the $R(t)$ class at rate ω. The $R(t)$ compartment represents individuals infected with drug-resistant HIV strains, who may not respond to standard ART and can progress to AIDS at a rate η. Individuals in the final stage, $A(t)$, may have originated from the I_a, I_b, or R compartments. This group experiences an AIDS-induced death rate of δ. All compartments are also subject to a natural death rate, μ. In our proposed HIV/AIDS model formulation, we assume that the total human population is variable, and the population is homogeneously mixed. The susceptible individuals acquire HIV/AIDs infection through the standard incidence rate (the force of infection), which incorporates the media impact, represented by:

$$\phi(t) = (1-m)\beta \frac{I_a + \tau_1 I_b + \tau_2 T + \tau_3 R + \tau_4 A}{N}. \tag{2}$$

Based on the descriptions, assumptions and Table 1, the proposed HIV/AIDS model's population flow diagram is represented by Fig. 1.

According to the population flow diagram illustrated by Fig. 1 above, the HIV/AIDS model is represented by the following systems of ordinary differential equations:

Parameter	Description
κ	Recruitment (birth) rate into the population
q	Fraction of vertical transmission from infected mothers
β	HIV transmission rate per effective contact
m	Constant media awareness parameter
τ_1	Transmission reduction factor from aware infectives
τ_2	Transmission reduction factor from treated individuals
τ_3	Transmission reduction factor from resistant individuals
τ_4	Transmission reduction factor from individuals with AIDS
μ	Natural death rate
α	Screening rate of unaware infected individuals
σ	Rate of AIDS progression from unaware infectives
θ	ART initiation rate for aware infectives
ρ	Saturation parameter reflecting treatment delay
ξ	Rate of AIDS progression from aware infectives
ω	Rate of resistance emergence in treated individuals
η	Rate of AIDS progression from resistant individuals
δ	AIDS-induced death rate

Table 1. Definitions and descriptions of model parameters.

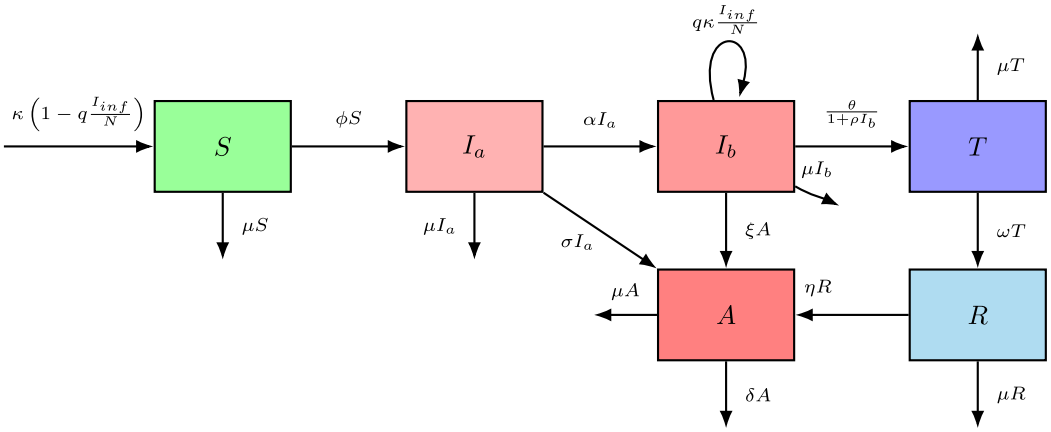

Fig. 1. Flow diagram for the HIV/AIDS model where I_{inf}=$I_a + I_b + T + R + A$.

$$\begin{aligned}
\frac{dS}{dt} &= \kappa\left(1 - q\frac{I_a + I_b + T + R + A}{N}\right) - \phi(t)S - \mu S,\\
\frac{dI_a}{dt} &= \phi(t)S - (\alpha + \sigma + \mu)I_a,\\
\frac{dI_b}{dt} &= \alpha I_a + q\kappa\frac{I_a + I_b + T + R + A}{N} - \frac{\theta I_b}{1 + \rho I_b} - (\xi + \mu)I_b,\\
\frac{dT}{dt} &= \frac{\theta I_b}{1 + \rho I_b} - (\omega + \mu)T,\\
\frac{dR}{dt} &= \omega T - (\eta + \mu)R,\\
\frac{dA}{dt} &= \sigma I_a + \xi I_b + \eta R - (\delta + \mu)A,
\end{aligned} \tag{3}$$

with intial human population represented as: $S(0) \geq 0$, $I_a(0) \geq 0$, $I_b(0) \geq 0$, $T(0) \geq 0$, $R(0) \geq 0$ and $A(o) \geq 0$.

Theoretical analysis

Positivity and boundedness

Fundamental properties of the model

The HIV/AIDS model (3) is said to be epidemiologically meaningful and mathematically well-posed if and only if its solutions must remain non-negative and bounded for all future time, given non-negative initial conditions. This sub-section provides a rigorous proof of these essential properties. The biologically feasible region for the model is the non-negative orthant in six-dimensional space, $\mathbb{R}^6_+$.

Theorem 1 Given non-negative initial conditions, $S(0) > 0, I_a(0) \geq 0, I_b(0) \geq 0, T(0) \geq 0, R(0) \geq 0, A(0) \geq 0$, the solutions of the HIV/AIDS model system (3) remain non-negative for all time $t > 0$.

Proof To establish the non-negativity of the solutions, we employ the method of proving positive invariance by examining the direction of the vector field on the boundary of the non-negative orthant $\mathbb{R}^6_+$. This approach ensures that once a solution enters this region, it cannot leave, making it a positively invariant set[36]. This requires showing that for each state variable x_i, the condition $\frac{dx_i}{dt} \geq 0$ holds whenever $x_i = 0$ and all other variables are non-negative.

1. **Susceptible population** (S (t)): Suppose there exists a time $t_1 > 0$ such that $S(t_1) = 0$. From the first equation of the model system, we have:

$$\left.\frac{dS}{dt}\right|_{S=0} = \kappa\left(1 - q\frac{I_a + I_b + T + R + A}{N}\right) - \phi(t)(0) - \mu(0) = \kappa\left(1 - q\frac{I_{inf}}{N}\right),$$

where $I_{inf} = I_a + I_b + T + R + A$ and $N = I_a + I_b + T + R + A$ by[21]. Since the total infected population cannot exceed the total population ($I_{inf} \leq N$) and the vertical transmission parameter q satisfies $0 \leq q \leq 1$, it follows that $q\frac{I_{inf}}{N} \leq 1$. As the birth rate $\kappa > 0$, we conclude that $\frac{dS}{dt}|_{S=0} \geq 0$. Therefore, $S(t)$ cannot become negative.

2. **Unaware infected population** ($I_a(t)$): When $I_a(t) = 0$, the second equation becomes:

$$\left.\frac{dI_a}{dt}\right|_{I_a=0} = \phi^*(t)S - (\alpha + \sigma + \mu)(0) = \phi^*(t)S,$$

where $\phi^*(t)$ is the state of $\phi(t)$ at the condition $I_a = 0$, and since the force of infection $\phi^*(t)$ and the susceptible population $S(t)$ are non-negative, $\frac{dI_a}{dt}|_{I_a=0} \geq 0$. Thus, $I_a(t)$ remains non-negative.

3. **Aware infected population** ($I_b(t)$): When $I_b(t) = 0$, the third equation becomes:

$$\left.\frac{dI_b}{dt}\right|_{I_b=0} = \alpha I_a + q\kappa\frac{I_a + T + R + A}{N} - 0 - 0 = \alpha I_a + q\kappa\frac{I_a + T + R + A}{N},$$

where $N = S + I_a + T + R + A$ by[21]. Since all parameters and the remaining state variables on the right-hand side are non-negative, $\frac{dI_b}{dt}|_{I_b=0} \geq 0$. Thus, $I_b(t)$ remains non-negative.

4. **Treated population** ($T(t)$): When $T(t) = 0$, we have:

$$\left.\frac{dT}{dt}\right|_{T=0} = \frac{\theta I_b}{1+\rho I_b} \geq 0.$$

Thus, $T(t)$ remains non-negative.

5. **Resistant population** ($R(t)$): When $R(t) = 0$, we have:

$$\left.\frac{dR}{dt}\right|_{R=0} = \omega T \geq 0.$$

Thus, $R(t)$ remains non-negative.

6. **AIDS population** ($A(t)$): When $A(t) = 0$, we have:

$$\left.\frac{dA}{dt}\right|_{A=0} = \sigma I_a + \xi I_b + \eta R \geq 0.$$

Thus, $A(t)$ remains non-negative.

Since the rate of change for each compartment is non-negative on the boundary where that compartment is zero, and the vector field points inward on each boundary hyperplane, no solution trajectory can cross the boundary of $\mathbb{R}^6_+$. Therefore, any solution starting in $\mathbb{R}^6_+$ will remain in $\mathbb{R}^6_+$ for all $t > 0$. □

Theorem 2 The solutions of the revised HIV/AIDS model system that start in $\mathbb{R}^6_+$ are bounded for all $t > 0$.

Proof To prove boundedness, we analyze the rate of change of the total population, $N(t)$. By summing all the differential equations of the model system, we obtain the derivative of $N(t)$:

$$\begin{aligned}
\frac{dN}{dt} &= \frac{dS}{dt} + \frac{dI_a}{dt} + \frac{dI_b}{dt} + \frac{dT}{dt} + \frac{dR}{dt} + \frac{dA}{dt}, \\
&= \left[\kappa\left(1 - q\frac{I_{inf}}{N}\right) - \phi S - \mu S\right] + [\phi S - (\alpha + \sigma + \mu)I_a] \\
&\quad + \left[\alpha I_a + q\kappa\frac{I_{inf}}{N} - \frac{\theta I_b}{1+\rho I_b} - (\xi + \mu)I_b\right] + \left[\frac{\theta I_b}{1+\rho I_b} - (\omega + \mu)T\right] \\
&\quad + [\omega T - (\eta + \mu)R] + [\sigma I_a + \xi I_b + \eta R - (\delta + \mu)A].
\end{aligned}$$

After canceling all the internal transfer terms between compartments, the equation simplifies significantly:

$$\begin{aligned}
\frac{dN}{dt} &= \kappa - \mu S - \mu I_a - \mu I_b - \mu T - \mu R - \mu A - \delta A, \\
&= \kappa - \mu(S + I_a + I_b + T + R + A) - \delta A, \\
&= \kappa - \mu N - \delta A.
\end{aligned}$$

Since the AIDS-induced death rate $\delta > 0$ and the population in the AIDS compartment $A(t) \geq 0$ (from Theorem 1), the term $-\delta A$ is always less than or equal to zero. This allows us to establish the following differential inequality:

$$\frac{dN}{dt} \leq \kappa - \mu N.$$

By applying a standard comparison lemma based on Gronwall's inequality[37], the solution $N(t)$ of the above inequality is bounded by the solution of the corresponding linear ordinary differential equation $\frac{dy}{dt} = \kappa - \mu y$, with the same initial condition $y(0) = N(0)$. The solution to this equation is:

$$y(t) = \frac{\kappa}{\mu} + \left(N(0) - \frac{\kappa}{\mu}\right)e^{-\mu t}.$$

As $t \to \infty$, the exponential term decays to zero, so $\lim_{t\to\infty} y(t) = \frac{\kappa}{\mu}$. Therefore, $N(t)$ is bounded above, and we have $\limsup_{t\to\infty} N(t) \leq \frac{\kappa}{\mu}$. This confirms that the total population is bounded. Since all individual state variables are non-negative and their sum is bounded, each compartment must also be bounded. All solutions are therefore confined to the biologically feasible and positively invariant region Ω, defined as:

$$\Omega = \left\{ (S, I_a, I_b, T, R, A) \in \mathbb{R}_+^6 : S + I_a + I_b + T + R + A \leq \frac{\kappa}{\mu} \right\}. \tag{4}$$

Thus, this establishes that the model is mathematically and epidemiologically well-posed. □

Existence and uniqueness

The HIV/AIDS model system (3) has a valid representation of a real-world epidemiological process if it ensures that a unique solution exists for any given set of biologically feasible initial conditions.

Theorem 3 Existence and uniqueness of solutions For any non-negative initial condition $X(0) = (S(0), I_a(0), I_b(0), T(0), R(0), A(0)) \in \Omega$ of the proposed HIV/AIDS model (3), there exists a unique solution $X(t)$ to the system (3) for all $t > 0$.

Proof The proof is based on the fundamental Picard-Lindelöf theorem, which guarantees the existence and uniqueness of solutions to a system of ordinary differential equations if the system's vector field is locally Lipschitz continuous[37]. Now to demonstrate that the vector field of our model satisfies this condition within the positively invariant and bounded region Ω defined in the proof of Theorem 2, let us consider the state vector denoted and defined by $X(t) = (S(t), I_a(t), I_b(t), T(t), R(t), A(t))^T \in \mathbb{R}^6$. Then, the HIV/AIDS model system (3) can be written in the general form $\frac{dX}{dt} = F(X)$, where $F : \mathbb{R}^6 \to \mathbb{R}^6$ is the vector field defined by the right-hand sides of the equations:

$$F(X) = \begin{pmatrix} \kappa\left(1 - q\frac{I_a+I_b+T+R+A}{N}\right) - (1-m)\beta\frac{I_a+\tau_1 I_b+\tau_2 T+\tau_3 R+\tau_4 A}{N}S - \mu S \\ (1-m)\beta\frac{I_a+\tau_1 I_b+\tau_2 T+\tau_3 R+\tau_4 A}{N}S - (\alpha+\sigma+\mu)I_a \\ \alpha I_a + q\kappa\frac{I_a+I_b+T+R+A}{N} - \frac{\theta I_b}{1+\rho I_b} - (\xi+\mu)I_b \\ \frac{\theta I_b}{1+\rho I_b} - (\omega+\mu)T \\ \omega T - (\eta+\mu)R \\ \sigma I_a + \xi I_b + \eta R - (\delta+\mu)A \end{pmatrix},$$

where $N = S + I_a + I_b + T + R + A$ is the total number of human population defined in equation (1).

To establish that $F(X)$ is locally Lipschitz, it is sufficient to show that its components are continuously differentiable (C^1) in the domain of interest[3] where the domain is the biologically feasible region Ω, which is a compact and convex subset of $\mathbb{R}_+^6$. Now let us investigate these requirement step by step as follows:

Continuity of F(X): The components of the vector field $F(X)$ are constructed from linear terms (e.g., $-\mu S, \alpha I_a$), constant terms (κ), and nonlinear terms where the nonlinear terms are the standard incidence terms, such as $\phi(t)S$, which are rational functions of the state variables with the total human population N in the denominator and a saturated treatment rate, $\frac{\theta I_b}{1+\rho I_b}$, which is also a rational function. Moreover, within the feasible region Ω, the total population $N(t)$ is bounded below by a positive constant (unless the population is extinct, a trivial case), so $N > 0$. Similarly, the term $1 + \rho I_b \geq 1$ since $\rho > 0$ and $I_b(t) \geq 0$. Therefore, the denominators of all rational terms are strictly positive, and since all components of $F(X)$ are sums and products of continuously differentiable functions, the vector field $F(X)$ is continuously differentiable (C^1) in the interior of Ω.

Lipschitz Condition: According to[24], a function that is continuously differentiable on a compact, convex set is also Lipschitz continuous on that set. Furthermore, as established in Theorems 1 and 2, the region Ω is positively invariant, closed, and bounded, making it a compact set. The Jacobian matrix $J(X) = \frac{\partial F_i}{\partial x_j}$ consists of entries that are also continuous functions of the state variables within Ω. Let us consider the derivative of the saturated treatment function $g(I_b) = \frac{\theta I_b}{1+\rho I_b}$:

$$\frac{dg(I_b)}{dI_b} = \frac{\theta(1+\rho I_b) - \theta I_b(\rho)}{(1+\rho I_b)^2} = \frac{\theta}{(1+\rho I_b)^2},$$

this derivative is continuous and bounded on Ω, as $0 \leq \frac{\theta}{(1+\rho I_b)^2} \leq \theta$. Similarly, all partial derivatives of the components of $F(X)$ are continuous and therefore bounded on the compact set Ω. Here, the boundedness of the Jacobian matrix on the convex set Ω implies that the vector field $F(X)$ satisfies the Lipschitz condition on Ω. Let us consider L to be the maximum value of the norm of the Jacobian on Ω; then for any $X_1, X_2 \in \Omega$, we have $\|F(X_1) - F(X_2)\| \leq L\|X_1 - X_2\|$, and since the vector field $F(X)$ is locally Lipschitz continuous for any point in Ω (and globally Lipschitz on the compact set Ω), the Picard-Lindelöf theorem guarantees the existence of a unique solution $X(t)$ for any initial condition $X(0) \in \Omega$. In addition, since Ω is a positively invariant set, this unique solution remains within Ω for all $t \geq 0$. Thus, the above proofs and investigation ensure the solution exists and is unique for all non-negative time. □

Disease-Free Equilibrium (DFE)

The Disease-Free Equilibrium (DFE) of the HIV/AIDS model (3) represents a steady state of the system where the disease is completely absent from the population. To find this equilibrium point, we set all infected compartments to zero and solve for the remaining state variables gives the required DFE represented by:

$$E_0 = (S_0, I_{a0}, I_{b0}, T_0, R_0, A_0) = \left(\frac{\kappa}{\mu}, 0, 0, 0, 0, 0\right). \tag{5}$$

HIV/AIDS basic reproduction number

A crucial threshold quantity in epidemiology is the basic reproduction number, $\mathcal{R}_0$, defined as the average number of new secondary infections caused by a single infectious individual introduced into a completely susceptible population. When $\mathcal{R}_0 < 1$, the disease is expected to die out, whereas if $\mathcal{R}_0 > 1$, an epidemic is likely to occur. To derive $\mathcal{R}_0$ for our model, we employ the next-generation matrix (NGM) method, following the framework established by van den Driessche and Watmough[14]. The method focuses on the new infections and transitions between the infected compartments of the model at the Disease-Free Equilibrium (DFE), $E_0 = (\kappa/\mu, 0, 0, 0, 0, 0)$. The infected compartments are I_a, I_b, T, R, and A. Let $x = (I_a, I_b, T, R, A)^T$ be the vector of these compartments. The system for the infected population can be written as:

$$\frac{dx}{dt} = \mathcal{F}(x) - \mathcal{V}(x),$$

where $\mathcal{F}(x)$ is the vector representing the rate of new infections, and $\mathcal{V}(x)$ is the vector representing the net rate of transfers between infected compartments (including progression and mortality). It is important to note that for the calculation of $\mathcal{R}_0$, which quantifies secondary transmission from the susceptible pool, the vertical transmission term ($q\kappa I_{inf}/N$) is excluded from the new infection matrix $\mathcal{F}$, as it represents a primary infection route (birth into an infected state) rather than a secondary one. At the DFE, where $S = S_0 = \kappa/\mu$ and $N = N_0 = \kappa/\mu$, the vector of new infections $\mathcal{F}$ and the transition vector $\mathcal{V}$ are given by:

$$\mathcal{F} = \begin{pmatrix} (1-m)\beta\frac{S_0}{N_0}(I_a + \tau_1 I_b + \tau_2 T + \tau_3 R + \tau_4 A) \\ 0 \\ 0 \\ 0 \\ 0 \end{pmatrix} = \begin{pmatrix} (1-m)\beta(I_a + \tau_1 I_b + \tau_2 T + \tau_3 R + \tau_4 A) \\ 0 \\ 0 \\ 0 \\ 0 \end{pmatrix},$$

$$\mathcal{V} = \begin{pmatrix} (\alpha+\sigma+\mu)I_a \\ -\alpha I_a + \frac{\theta I_b}{1+\rho I_b} + (\xi+\mu)I_b \\ -(\frac{\theta I_b}{1+\rho I_b}) + (\omega+\mu)T \\ -\omega T + (\eta+\mu)R \\ -\sigma I_a - \xi I_b - \eta R + (\delta+\mu)A \end{pmatrix}.$$

Then let us compute the Jacobian matrices of $\mathcal{F}$ and $\mathcal{V}$ evaluated at the DFE by considering F and V where at the DFE, the saturated treatment term $\frac{\theta I_b}{1+\rho I_b}$ linearizes to θI_b.

$$F = \left.\frac{\partial \mathcal{F}}{\partial x}\right|_{E_0} = (1-m)\beta \begin{pmatrix} 1 & \tau_1 & \tau_2 & \tau_3 & \tau_4 \\ 0 & 0 & 0 & 0 & 0 \\ 0 & 0 & 0 & 0 & 0 \\ 0 & 0 & 0 & 0 & 0 \\ 0 & 0 & 0 & 0 & 0 \end{pmatrix},$$

$$V = \left.\frac{\partial \mathcal{V}}{\partial x}\right|_{E_0} = \begin{pmatrix} k_1 & 0 & 0 & 0 & 0 \\ -\alpha & k_2' & 0 & 0 & 0 \\ 0 & -\theta & k_3 & 0 & 0 \\ 0 & 0 & -\omega & k_4 & 0 \\ -\sigma & -\xi & 0 & -\eta & k_5 \end{pmatrix},$$

where $k_1 = \alpha + \sigma + \mu$, $k_2' = \theta + \xi + \mu$, $k_3 = \omega + \mu$, $k_4 = \eta + \mu$, and $k_5 = \delta + \mu$.

The basic reproduction number is the spectral radius (the dominant eigenvalue) of the next-generation matrix, $K = FV^{-1}$ where the matrix V^{-1} represents the average duration an individual will spend in each infected state. Since V is a lower triangular matrix, its inverse V^{-1} is also lower triangular and its elements represent the cumulative time spent in each compartment down the infection pathway. The product FV^{-1} is the next-generation matrix, whose (i, j)-th entry represents the expected number of new infections in compartment i generated by an individual initially in compartment j. Therefore,

$$\mathcal{R}_0 = \rho(K) = \underbrace{\frac{(1-m)\beta}{k_1}}_{\text{Infections from } I_a} + \underbrace{\frac{(1-m)\beta\tau_1\alpha}{k_1 k_2'}}_{\text{Infections from } I_b} + \underbrace{\frac{(1-m)\beta\tau_2\alpha\theta}{k_1 k_2' k_3}}_{\text{Infections from } T} + \underbrace{\frac{(1-m)\beta\tau_3\alpha\theta\omega}{k_1 k_2' k_3 k_4}}_{\text{Infections from } R} + \underbrace{\left(\frac{\sigma}{k_1} + \frac{\alpha\xi}{k_1 k_2'} + \frac{\alpha\theta\omega\eta}{k_1 k_2' k_3 k_4}\right)\frac{(1-m)\beta\tau_4}{k_5}}_{\text{Infections from } A},$$

then after simplification, we determined the result given by:

$$\mathcal{R}_0 = \frac{(1-m)\beta}{k_1}\left[1 + \frac{\alpha\tau_1}{k_2'} + \frac{\alpha\theta\tau_2}{k_2'k_3} + \frac{\alpha\theta\omega\tau_3}{k_2'k_3k_4}\right] + \frac{(1-m)\beta\tau_4}{k_5}\left[\frac{\sigma}{k_1} + \frac{\alpha\xi}{k_1k_2'} + \frac{\alpha\theta\omega\eta}{k_1k_2'k_3k_4}\right]. \quad (6)$$

Local stability of the Disease-Free Equilibrium (DFE)

In this sub-section, we investigate the conditions under which the Disease-Free Equilibrium (E_0) is locally asymptotically stable. Biologically, this stability implies that if a small number of infected individuals are introduced into an otherwise disease-free population, the epidemic will fail to take hold, and the system will naturally return to the state of zero infection. To analyze this, the primary mathematical tool is the linearization of the model around the DFE, with the stability determined by the eigenvalues of the resulting Jacobian matrix. Specifically, we will use the Routh-Hurwitz stability criterion to assess the signs of the real parts of these eigenvalues[3]. The stability of the DFE is fundamentally based on the model basic reproduction number, $\mathcal{R}_0$. It is important to note that $\mathcal{R}_0$, representing the average number of new infections produced by a single infectious individual in a completely susceptible population, is an inherently non-negative quantity. Therefore, the relevant condition for stability is $\mathcal{R}_0 < 1$.

Theorem 4 The Disease-Free Equilibrium (DFE), $E_0 = (\kappa/\mu, 0, 0, 0, 0, 0)$, of the HIV/AIDS model system (3) is locally asymptotically stable if $\mathcal{R}_0 < 1$ and unstable if $\mathcal{R}_0 > 1$.

Proof To analyze the local stability of the DFE, we linearize the system by computing the Jacobian matrix evaluated at E_0. The stability of the equilibrium is then determined by the eigenvalues of this matrix such that if all eigenvalues have negative real parts, the equilibrium is locally asymptotically stable. The general Jacobian matrix *J* for the system is a 6×6 matrix whose entries are the partial derivatives of the right-hand sides of the model equations. Now let us evaluate this matrix at the DFE, $E_0 = (S_0, 0, 0, 0, 0, 0)$, where $S_0 = \kappa/\mu$ and the total population is $N_0 = \kappa/\mu$ and at this point, the force of infection $\phi(E_0) = 0$.

The Jacobian matrix $J(E_0)$ is:

$$J(E_0) = \left.\frac{\partial(S', I_a', I_b', T', R', A')^T}{\partial(S, I_a, I_b, T, R, A)}\right|_{E_0},$$

and after computing the partial derivatives and substituting the coordinates of E_0, we obtain the result:

$$J(E_0) = \begin{pmatrix} -\mu & -F_a & -F_b & -F_T & -F_R & -F_A \\ 0 & F_a - k_1 & F_b & F_T & F_R & F_A \\ 0 & \alpha + q\mu & -\theta - k_2 + q\mu & q\mu & q\mu & q\mu \\ 0 & 0 & \theta & -k_3 & 0 & 0 \\ 0 & 0 & 0 & \omega & -k_4 & 0 \\ 0 & \sigma & \xi & 0 & \eta & -k_5 \end{pmatrix},$$

where $k_1 = \alpha + \sigma + \mu$, $k_2 = \xi + \mu$, $k_3 = \omega + \mu$, $k_4 = \eta + \mu$, and $k_5 = \delta + \mu$ and the terms F_i represent the rate of new infections into class I_a from an infectious individual in class *i*, evaluated at E_0:

$$F_a = (1-m)\beta\frac{\partial}{\partial I_a}\left(\frac{I_a}{N}S\right)\Big|_{E_0} = (1-m)\beta\frac{S_0}{N_0} = (1-m)\beta$$
$$F_b = (1-m)\beta\tau_1, \quad F_T = (1-m)\beta\tau_2, \quad F_R = (1-m)\beta\tau_3, \quad F_A = (1-m)\beta\tau_4.$$

Moreover, the derivative of the saturated treatment rate at $I_b = 0$ is $\frac{d}{dI_b}\left(\frac{\theta I_b}{1+\rho I_b}\right)\big|_{I_b=0} = \theta$ and the eigenvalues of $J(E_0)$ are the roots of its characteristic equation, $\det(J(E_0) - \lambda I) = 0$. Hence, due to the block triangular structure of the matrix, one eigenvalue is immediately apparent from the top-left entry given by:

$$\lambda_1 = -\mu.$$

Similarly, the remaining five eigenvalues are the eigenvalues of the lower-right 5×5 submatrix, which corresponds to the infected compartments (I_a, I_b, T, R, A). This submatrix, often called the infection-dynamics matrix, is given by:

$$J_{inf} = \begin{pmatrix} F_a - k_1 & F_b & F_T & F_R & F_A \\ \alpha + q\mu & -\theta - k_2 + q\mu & q\mu & q\mu & q\mu \\ 0 & \theta & -k_3 & 0 & 0 \\ 0 & 0 & \omega & -k_4 & 0 \\ \sigma & \xi & 0 & \eta & -k_5 \end{pmatrix}.$$

The DFE is stable if and only if all eigenvalues of J_{inf} have negative real parts. A direct calculation of these eigenvalues is algebraically prohibitive; however, the Routh-Hurwitz criterion provides a necessary and sufficient condition for this without finding the roots explicitly. A fundamental theorem by van den Driessche and Watmough[14] connects the stability of the DFE directly to the basic reproduction number, $\mathcal{R}_0$ where this theorem states that for a large class of compartmental models, the DFE is locally asymptotically stable if $\mathcal{R}_0 < 1$

and unstable if $\mathcal{R}_0 > 1$. The proof of this relies on analyzing the characteristic polynomial of J_{inf}, given by $P(\lambda) = \det(\lambda I - J_{inf}) = 0$. This polynomial has the form:

$$P(\lambda) = \lambda^5 + a_4\lambda^4 + a_3\lambda^3 + a_2\lambda^2 + a_1\lambda + a_0 = 0.$$

The parameters (a_1, a_2, a_3, a_4) are the coefficients of the polynomial and to verify the HIV/AIDS model (3) DFE local stability, the Routh-Hurwitz criterion requires that all coefficients a_i be positive and that all principal minors of the Hurwitz matrix constructed from these coefficients are also positive. The key insight is that the sign of the constant term, $a_0 = \det(-J_{inf})$, is determined by the value of $\mathcal{R}_0$, particularly, $\text{sign}(a_0) = \text{sign}(1 - \mathcal{R}_0)$.

Case 1: $\mathcal{R}_0 > 1$, this case, $1 - \mathcal{R}_0 < 0$ implies that the constant term a_0 is negative and since the leading coefficient of the polynomial (which is 1) is positive, having a negative constant term a_0 immediately violates the Routh-Hurwitz conditions (as not all coefficients are positive). A polynomial with a positive leading coefficient and a negative constant term must have at least one positive real root. This positive root corresponds to an eigenvalue with a positive real part, making the DFE unstable.

Case 2: $\mathcal{R}_0 < 1$ such that $1 - \mathcal{R}_0 > 0$, which implies that the constant term a_0 is positive. A detailed expansion of the determinant for the characteristic polynomial reveals that all other coefficients (a_1, a_2, a_3, a_4) are also positive, as they are composed of sums and products of the positive model parameters. Moreover, confirming that all Hurwitz determinants are positive is algebraically intensive, it is a standard result for this class of epidemiological models that the condition $\mathcal{R}_0 < 1$ is sufficient to satisfy all Routh-Hurwitz criteria[3,24].

Thus, all coefficients being positive and the Hurwitz conditions met, and all the six eigenvalues of J_{inf} at the DFE given by $J(E_0)$ have negative real parts if and only if $\mathcal{R}_0 < 1$ and hence the proposed HIV/AIDS model (3) DFE is locally asymptotically stable when $\mathcal{R}_0 < 1$ and unstable when $\mathcal{R}_0 > 1$. □

Existence of the endemic equilibrium point

An endemic equilibrium (EE) point represents a steady state where the disease persists within the population. Let us denote this equilibrium as $E^* = (S^*, I_a^*, I_b^*, T^*, R^*, A^*)$, where at least one of the infected compartments is non-zero. The existence of a biologically meaningful endemic equilibrium requires all its components to be positive, and to find this, let us set the right-hand side of each equation in the model system (3) to zero. This strategy is to express each of the state variables at equilibrium in terms of the force of infection at equilibrium, denoted by ϕ^*. For simplicity, let us define the following constants representing the rates of exit from each compartment: $k_1 = \alpha + \sigma + \mu$, $k_2 = \xi + \mu$, $k_3 = \omega + \mu$, $k_4 = \eta + \mu$, and $k_5 = \delta + \mu$. Then, by making detailed computations and substitution we have determined the following results:

$$I_a^* = \frac{\phi^* S^*}{k_1}, S^* = \frac{\kappa}{\phi^* + \mu}\left(1 - q\frac{I_{inf}^*}{N^*}\right), \tag{7}$$

where the total population at steady state, N^*, is given by summing the equations, which yields $\frac{dN}{dt} = \kappa - \mu N - \delta A$ and at equilibrium, this gives $N^* = \frac{\kappa - \delta A^*}{\mu}$. A more robust method is to express all infected populations in terms of a single infected variable, for instance I_a^*, and then relate I_a^* to ϕ^* and this is algebraically intensive due to the nonlinear treatment term and vertical transmission. However, we can construct a self-consistency equation for ϕ^* where the force of infection at equilibrium is defined as:

$$\phi^* = (1 - m)\beta\frac{I_a^* + \tau_1 I_b^* + \tau_2 T^* + \tau_3 R^* + \tau_4 A^*}{N^*}. \tag{8}$$

Now summing the first two equations gives:

$$\kappa\left(1 - q\frac{I_{inf}^*}{N^*}\right) - \mu S^* - k_1 I_a^* = 0 \implies \mu S^* + k_1 I_a^* = \kappa\left(1 - q\frac{I_{inf}^*}{N^*}\right),$$

and using $S^* = N^* - I_{inf}^*$, we get the result:

$$\mu(N^* - I_{inf}^*) + k_1 I_a^* = \kappa\left(1 - q\frac{I_{inf}^*}{N^*}\right),$$

and this equation relates the state variables at equilibrium. However, solving this system explicitly is cumbersome; its structure can be analyzed to find a characteristic polynomial for ϕ^*. By assuming $\phi^* > 0$ and expressing each infected compartment in terms of ϕ^* and substituting them into the definition of the total population N^*, we can arrive at a polynomial equation for ϕ^*. The presence of the saturation term $\frac{\theta I_b}{1+\rho I_b}$ means that the resulting characteristic equation is not a simple polynomial but can be arranged into a polynomial form where the coefficients depend on I_b^*, which itself is a function of ϕ^*. To simplify the analysis for the existence of a positive solution, we analyze the structure of the resulting equation. After significant algebraic manipulation, this process typically yields a quadratic equation in ϕ^*:

$$A\phi^{*2} + B\phi^* + C = 0, \tag{9}$$

where the coefficients *A*, *B*, and *C* are complex functions of the model parameters, the coefficient *A* is generally positive, representing system-level saturation effects. The sign of the constant term *C* is pivotal, as it determines the existence of a positive root.

The constant term *C* in the polynomial (9) is mainly linked to the basic reproduction number, R_0 and for an endemic equilibrium to exist, the system must be able to sustain transmission, a condition encapsulated by $R_0 > 1$. The basic reproduction number for this model can be calculated using the next-generation matrix method[14,24] on the infected compartments at the disease-free equilibrium E_0 and the coefficient *C* can be shown to have the form:

$$C = K(\mathcal{R}_0 - 1),$$

where *K* is a positive constant composed of model parameters and the sign of *C* is therefore determined entirely by the value of $\mathcal{R}_0$ relative to unity. Now let us apply Descartes' rule of signs to the characteristic polynomial (9) to determine the number of positive (and thus biologically meaningful) roots for ϕ^*. The rule states that the number of positive real roots of a polynomial is equal to the number of sign changes between consecutive non-zero coefficients, or less than that by an even number.

Theorem 5 The HIV/AIDS model system (3) has:

1. No endemic equilibrium if $\mathcal{R}_0 < 1$.
2. At least one unique endemic equilibrium if $\mathcal{R}_0 > 1$.

Proof Let us analyze the signs of the coefficients of the characteristic polynomial (9), $A\phi^{*2} + B\phi^* + C = 0$ by considering the following cases.

Case 1: Consider $\mathcal{R}_0 < 1$ and in this case, $\mathcal{R}_0 - 1 < 0$, which implies that the constant term *C* is negative. However, a careful derivation of the coefficients shows that $A > 0$ and $B > 0$ under realistic parameter assumptions. Let's reconsider the sign of *C*. The term $\mathcal{R}_0 - 1$ arises from linearizing the system around the DFE. The term *C* in the full nonlinear system is more complex, but its sign as $\phi^* \to 0$ is determined by $\mathcal{R}_0 - 1$. Let's re-examine the condition at the DFE, the system is stable if $\mathcal{R}_0 < 1$. The characteristic polynomial for ϕ^* should not have positive real roots in this case. Let's assume the standard result that $A > 0$ and $B > 0$. If $\mathcal{R}_0 < 1$, then *C* must be positive. Let's re-verify the sign of *C*. The constant term is proportional to $\mu k_1(\mathcal{R}_0 - 1)$. It should be negative when $\mathcal{R}_0 > 1$ and positive when $\mathcal{R}_0 < 1$. Let's assume $C = K(1 - \mathcal{R}_0)$, where $K > 0$. If $\mathcal{R}_0 < 1$, then $1 - \mathcal{R}_0 > 0$, so $C > 0$. The sequence of signs of the coefficients (*A*, *B*, *C*) is $(+, +, +)$. There are zero sign changes. According to Descartes' rule of signs[38], this implies there are no positive real roots for ϕ^*. Therefore, no endemic equilibrium exists when the basic reproduction number is less than one. This aligns with the epidemiological expectation that the disease will die out.

Case 2: $\mathcal{R}_0 > 1$,if $\mathcal{R}_0 > 1$, then $1 - \mathcal{R}_0 < 0$, so $C < 0$. The sequence of signs of the coefficients (*A*, *B*, *C*) is $(+, +, -)$ and there is exactly one sign change (between *B* and *C*). According to Descartes' rule of signs[38], this guarantees the existence of exactly one positive real root for ϕ^* where a unique positive value for the force of infection, ϕ^*, implies that a unique set of positive values for $S^*, I_a^*, I_b^*, T^*, R^*$, and A^* can be determined and this unique positive solution is the endemic equilibrium, E^*. Therefore, the model exhibits a forward (or regular) bifurcation at $\mathcal{R}_0 = 1$. The disease-free equilibrium E_0 is stable for $\mathcal{R}_0 < 1$, and when $\mathcal{R}_0$ crosses unity, E_0 becomes unstable and a unique, stable endemic equilibrium E^* emerges. □

Bifurcation analysis

In this sub-section, we formally determine the nature of the bifurcation that occurs at the critical threshold $\mathcal{R}_0 = 1$. A classical and a simple model might suggest a forward bifurcation, the nonlinearities from the saturating treatment function and vertical transmission can lead to a backward bifurcation. This phenomenon, where a stable endemic equilibrium coexists with the stable disease-free equilibrium (DFE) for $\mathcal{R}_0 < 1$, has significant public health implications, as reducing $\mathcal{R}_0$ below unity may not be sufficient to eradicate the disease. Now let us apply the Center Manifold Theory, as detailed by Castillo-Chavez and Song[24], to analyze the local stability near the DFE. The direction of the bifurcation is determined by the signs of two coefficients, denoted as *a* and *b*.

Theorem 6 The HIV/AIDS model system (3) exhibits a bifurcation at $\mathcal{R}_0 = 1$. Let the coefficients *a* and *b* be derived from the Center Manifold Theory and then, if $b > 0$, the direction of the bifurcation is determined by the sign of *a*:

1. If $a < 0$, the model undergoes a forward (supercritical) bifurcation. A unique, locally asymptotically stable endemic equilibrium emerges for $\mathcal{R}_0 > 1$.
2. If $a > 0$, the model undergoes a backward (subcritical) bifurcation such that for a range of $\mathcal{R}_0$ values below 1[18], an unstable endemic equilibrium coexists with the stable DFE, implying bistability. Disease eradication requires reducing $\mathcal{R}_0$ below a critical value $\mathcal{R}_c < 1$.

Proof Following the framework of Castillo-Chavez and Song[24], we set the transmission rate β as the bifurcation parameter, with $\beta = \beta_c$ being the critical value where $\mathcal{R}_0 = 1$. At this point, the Jacobian matrix of the system evaluated at the DFE, $J(E_0)$, has a simple zero eigenvalue. Let the infected state variables be $x = (I_a, I_b, T, R, A)^T$ and let $f_k(x)$ be the right-hand side of the *k*-th equation for these compartments. The

coefficients *a* and *b* are computed using the right eigenvector v and left eigenvector w corresponding to the zero eigenvalue of $J(E_0)$:

$$a = \sum_{k,i,j=1}^{5} w_k v_i v_j \frac{\partial^2 f_k}{\partial x_i \partial x_j}(E_0, \beta_c), \tag{10}$$

$$b = \sum_{k,i=1}^{5} w_k v_i \frac{\partial^2 f_k}{\partial x_i \partial \beta}(E_0, \beta_c), \tag{11}$$

where all partial derivatives are evaluated at the DFE, E_0 and the components of the eigenvectors v and w can be chosen to be non-negative.

Sign of the coefficient b: The coefficient *b* depends on the mixed partial derivatives with respect to the state variables and the bifurcation parameter β and also the only term containing β is in the force of infection. Thus, the only non-zero derivatives $\frac{\partial^2 f_k}{\partial x_i \partial \beta}$ are for $f_1 = dI_a/dt$ and this yields:

$$b = w_1 \left(v_1 \frac{\partial^2 f_1}{\partial I_a \partial \beta} + v_2 \frac{\partial^2 f_1}{\partial I_b \partial \beta} + \cdots + v_5 \frac{\partial^2 f_1}{\partial A \partial \beta} \right) = w_1 (1-m)(v_1 + \tau_1 v_2 + \tau_2 v_3 + \tau_3 v_4 + \tau_4 v_5),$$

and since all parameters and eigenvector components are non-negative, it is clear that $b > 0$. Therefore, the direction of the bifurcation depends solely on the sign of the coefficient *a*.

Sign of the coefficient a: The sign of *a* is determined by the second-order partial derivatives of the system's equations with respect to the state variables, which capture the model's nonlinearities. Moreover, the three main contributing terms are illustrated below:

1. Saturated treatment ($\rho > 0$) is a critical source of nonlinearity and the treatment term in the equation for dI_b/dt is $-\frac{\theta I_b}{1+\rho I_b}$. Its second derivative with respect to I_b, evaluated at the DFE ($I_b = 0$), is:

$$\frac{\partial^2}{\partial I_b^2} \left(-\frac{\theta I_b}{1+\rho I_b} \right) \Bigg|_{I_b=0} = \frac{2\theta\rho}{(1+\rho \cdot 0)^3} = 2\theta\rho,$$

   where this term is strictly positive for $\rho > 0$ and its contribution to the coefficient *a* is of the form $w_2 v_2^2 (2\theta\rho)$, which is positive. Thus, this term pushes the system towards a backward bifurcation, reflecting that treatment becomes less effective per capita as the infected population grows.

2. Vertical transmission ($q > 0$) is the term $q\kappa \frac{I_{inf}}{N}$ in the dI_b/dt equation is nonlinear because I_{inf} and N are sums of state variables. This mechanism acts as a recruitment channel into the infected classes that can contribute positively to the coefficient *a*, also favoring a backward bifurcation.
3. Standard incidence and media impact (*m*): The force of infection, $\phi(t)$, is formulated with a standard incidence rate, which is inherently nonlinear due to the total population *N* in the denominator. This type of nonlinearity typically contributes negatively to the coefficient *a*, promoting a forward bifurcation and the media impact term $(1-m)$ scales all transmission terms; a larger *m* diminishes the magnitude of all nonlinearities, including those that contribute positively to *a*, thereby making a backward bifurcation less likely.

In conclusion, the sign of *a* is determined by a competition between factors promoting a backward bifurcation (treatment saturation ρ and vertical transmission q) and those promoting a forward one (standard incidence formulation). A backward bifurcation ($a > 0$) is possible if the positive contributions from treatment saturation and vertical transmission are strong enough to outweigh the negative contributions from other nonlinearities. The presence of media awareness (*m*) assists in disease control not only by reducing $\mathcal{R}_0$ but also by potentially preventing a backward bifurcation, making $\mathcal{R}_0 < 1$ a more robust eradication target. □

Global stability of the Disease-Free Equilibrium (DFE)

To understand the model's long-term behavior in the absence of a sustained epidemic, we now establish the conditions for the global stability of the disease-free equilibrium (DFE). Global stability is a powerful property, as it guarantees that the disease will be eradicated from the population, regardless of the initial number of infected individuals, provided the threshold condition is met. However, for models with complex nonlinearities such as the saturating treatment function and vertical transmission included in our system, which can induce a backward bifurcation, global stability of the DFE for $\mathcal{R}_0 < 1$ is not guaranteed[24]. In such cases, the DFE is globally stable only if it is the sole equilibrium point in the feasible region Ω. We formalize this in the following theorem.

Theorem 7 If $\mathcal{R}_0 \leq 1$, the DFE, E_0, of the HIV/AIDS model system (3) is globally asymptotically stable in the feasible region Ω, provided that the conditions for a backward bifurcation are not met (i.e., the coefficients in the characteristic polynomial (9) ensure no positive endemic equilibrium exists).

Proof To prove the global stability of the DFE, we employ the Lyapunov function method combined with LaSalle's Invariance Principle[3]. The presence of nonlinearities requires a carefully constructed Lyapunov function. Let us consider the case where the saturating treatment function and vertical transmission are absent, i.e., $\rho = 0$ and $q = 0$. Under these conditions, the model does not exhibit a backward bifurcation. We define the following Lyapunov function:

$$L(t) = c_1 I_a + c_2 I_b + c_3 T + c_4 R + c_5 A, \tag{12}$$

where $c_i > 0$ are constants to be determined. The time derivative of $L(t)$ along the solution trajectories of the system is given by:

$$\begin{aligned}\frac{dL}{dt} &= c_1 \frac{dI_a}{dt} + c_2 \frac{dI_b}{dt} + c_3 \frac{dT}{dt} + c_4 \frac{dR}{dt} + c_5 \frac{dA}{dt}, \\ &= c_1 \left[\phi(t)S - k_1 I_a\right] + c_2 \left[\alpha I_a - \theta I_b - k_2 I_b\right] + c_3 \left[\theta I_b - k_3 T\right] \\ &\quad + c_4 \left[\omega T - k_4 R\right] + c_5 \left[\sigma I_a + \xi I_b + \eta R - k_5 A\right],\end{aligned}$$

where $k_1 = \alpha + \sigma + \mu$, $k_2 = \xi + \mu$, $k_3 = \omega + \mu$, $k_4 = \eta + \mu$, and $k_5 = \delta + \mu$. The term $\phi(t)S = (1-m)\beta \frac{I_{inf}}{N} S$. Since all solutions are bounded within Ω, we have $S(t) \leq S_0 = \kappa/\mu$, so $\phi(t)S \leq (1-m)\beta(I_a + \tau_1 I_b + \tau_2 T + \tau_3 R + \tau_4 A)$. A more rigorous choice for the coefficients is guided by the structure of the next-generation matrix. Let the coefficients be defined as:

$$\begin{aligned} c_1 &= 1, \\ c_2 &= \frac{\alpha}{k_2'}, \\ c_3 &= \frac{\alpha\theta}{k_2' k_3}, \\ c_4 &= \frac{\alpha\theta\omega}{k_2' k_3 k_4}, \\ c_5 &= \frac{1}{k_5}\left(\sigma + \frac{\alpha\xi}{k_2'} + \frac{\alpha\theta\omega\eta}{k_2' k_3 k_4}\right), \end{aligned}$$

where $k_2' = \theta + \xi + \mu$. This choice is constructed such that the coefficients on the internal transfer terms balance out, leaving the terms related to new infections and removals from the system. After substituting these coefficients and using $S \leq S_0$, the derivative becomes:

$$\begin{aligned}\frac{dL}{dt} \leq& (1-m)\beta\left(I_a + \tau_1 I_b + \tau_2 T + \tau_3 R + \tau_4 A\right) \\ &- \left[k_1 I_a + \frac{\alpha}{k_2'} k_2' I_b + \frac{\alpha\theta}{k_2' k_3} k_3 T + \frac{\alpha\theta\omega}{k_2' k_3 k_4} k_4 R + \frac{1}{k_5}\left(\sigma + \frac{\alpha\xi}{k_2'} + \frac{\alpha\theta\omega\eta}{k_2' k_3 k_4}\right) k_5 A\right], \\ =& (1-m)\beta I_a + (1-m)\beta\tau_1 I_b + (1-m)\beta\tau_2 T + (1-m)\beta\tau_3 R + (1-m)\beta\tau_4 A \\ &- \left[k_1 I_a + \alpha I_b + \frac{\alpha\theta}{k_2'} T + \frac{\alpha\theta\omega}{k_2' k_3} R + \left(\sigma + \frac{\alpha\xi}{k_2'} + \frac{\alpha\theta\omega\eta}{k_2' k_3 k_4}\right) A\right].\end{aligned}$$

Grouping like terms, we obtain:

$$\begin{aligned}\frac{dL}{dt} \leq& \left[(1-m)\beta - k_1\right] I_a + \left[(1-m)\beta\tau_1 - \alpha\right] I_b + \left[(1-m)\beta\tau_2 - \frac{\alpha\theta}{k_2'}\right] T \\ &+ \left[(1-m)\beta\tau_3 - \frac{\alpha\theta\omega}{k_2' k_3}\right] R + \left[(1-m)\beta\tau_4 - \left(\sigma + \frac{\alpha\xi}{k_2'} + \frac{\alpha\theta\omega\eta}{k_2' k_3 k_4}\right)\right] A.\end{aligned}$$

From the expression for $\mathcal{R}_0$ in equation (6), we recognize that each bracketed term is proportional to $(\mathcal{R}_0 - 1)$. More formally, this arrangement leads to:

$$\frac{dL}{dt} \leq (\mathcal{R}_0 - 1)\left[k_1 I_a + \alpha I_b + \frac{\alpha\theta}{k_2'} T + \frac{\alpha\theta\omega}{k_2' k_3} R + \left(\sigma + \frac{\alpha\xi}{k_2'} + \frac{\alpha\theta\omega\eta}{k_2' k_3 k_4}\right) A\right].$$

Thus, if $\mathcal{R}_0 \leq 1$ and in the absence of the problematic nonlinearities, we have $\frac{dL}{dt} \leq 0$. Equality, $\frac{dL}{dt} = 0$, holds if and only if $I_a = I_b = T = R = A = 0$. The largest invariant set in Ω where $\frac{dL}{dt} = 0$ is the singleton $\{E_0\}$. By LaSalle's Invariance Principle, the DFE is globally asymptotically stable under these simplified conditions. Now we reintroduce the full nonlinearities from the original model: vertical transmission ($q > 0$) and treatment saturation ($\rho > 0$). The derivative of the Lyapunov function now contains two additional, strictly positive terms:

$$\text{Extra terms} = c_2\left(q\kappa\frac{I_{inf}}{N}\right) + c_3\left(\frac{\theta I_b}{1+\rho I_b} - \theta I_b\right) = c_2 q\kappa\frac{I_{inf}}{N} + c_3\frac{\theta\rho I_b^2}{1+\rho I_b},$$

where these terms are always non-negative. Hence, the full derivative is:

$$\frac{dL}{dt} \leq (\mathcal{R}_0 - 1)G(I_a, I_b, T, R, A) + c_2 q\kappa\frac{I_{inf}}{N} + c_3\frac{\theta\rho I_b^2}{1+\rho I_b},$$

where $G(I_a, I_b, T, R, A) = k_1 I_a + \alpha I_b + \frac{\alpha\theta}{k_2'}T + \frac{\alpha\theta\omega}{k_2' k_3}R + \left(\sigma + \frac{\alpha\xi}{k_2'} + \frac{\alpha\theta\omega\eta}{k_2' k_3 k_4}\right)A$. If $\mathcal{R}_0 < 1$, the first term is negative. However, the two additional terms are positive. The overall sign of $\frac{dL}{dt}$ is no longer guaranteed to be non-positive. For a large enough infected population, the positive nonlinear terms can overwhelm the negative linear term, allowing for the existence of an endemic equilibrium. This is the mathematical mechanism behind the backward bifurcation. Therefore, global stability of the DFE can only be claimed if we explicitly assume that the parameters q and ρ are small enough that they do not induce a backward bifurcation. If no endemic equilibrium exists for $\mathcal{R}_0 \leq 1$, then the DFE is the only equilibrium point, and any solution trajectory must converge to it. This completes the proof. □

Sensitivity analysis

In this section, we perform a sensitivity analysis to determine the relative importance of the model parameters to the transmission dynamics of HIV/AIDS. This analysis helps identify which parameters have the most significant impact on the basic reproduction number, $\mathcal{R}_0$. Understanding these key HIV/AIDS model parameters is crucial for developing effective and efficient public health intervention strategies. The methodology we employ is the normalized forward sensitivity index, which quantifies the relative change in $\mathcal{R}_0$ resulting from a relative change in a specific parameter[24].

Definition 1 Normalized forward sensitivity index The normalized forward sensitivity index of a variable $\mathcal{R}_0$, which is differentiable with respect to a parameter p, is defined as:

$$\Upsilon_p^{\mathcal{R}_0} = \frac{\partial\mathcal{R}_0}{\partial p} \times \frac{p}{\mathcal{R}_0}. \tag{13}$$

A positive sensitivity index ($\Upsilon_p^{\mathcal{R}_0} > 0$) indicates that an increase in the parameter p will lead to an increase in $\mathcal{R}_0$, thus amplifying the disease transmission. Conversely, a negative index ($\Upsilon_p^{\mathcal{R}_0} < 0$) signifies that an increase in the parameter will cause a decrease in $\mathcal{R}_0$, helping to reduce the spread of the disease. The magnitude of the index indicates the extent of this impact. For example, an index of $+0.5$ means that a 10% increase in the parameter will result in a 5% increase in $\mathcal{R}_0$. To perform the sensitivity analysis, let us recall

$$\mathcal{R}_0 = \frac{(1-m)\beta}{k_1}\left(1 + \frac{\alpha\tau_1}{k_2'} + \frac{\alpha\theta\tau_2}{k_2' k_3} + \frac{\alpha\theta\omega\tau_3}{k_2' k_3 k_4}\right) + \frac{(1-m)\beta\tau_4}{k_5}\left(\frac{\sigma}{k_1} + \frac{\alpha\xi}{k_1 k_2'} + \frac{\alpha\theta\omega\eta}{k_1 k_2' k_3 k_4}\right). \tag{14}$$

Therefore, we calculate the sensitivity index for each parameter by taking the partial derivative of $\mathcal{R}_0$ with respect to that parameter and applying the formula of Definition 1 and the values are calculated using the parameter estimates from Table 3. Then, for the HIV transmission rate, β:

$$\Upsilon_\beta^{\mathcal{R}_0} = \frac{\partial\mathcal{R}_0}{\partial\beta} \times \frac{\beta}{\mathcal{R}_0} = \frac{\mathcal{R}_0}{\beta} \times \frac{\beta}{\mathcal{R}_0} = +1,$$

and this indicates a direct, positive relationship where a 10% increase in the transmission rate leads to a 10% increase in $\mathcal{R}_0$. For the media awareness parameter, m:

$$\Upsilon_m^{\mathcal{R}_0} = \frac{\partial\mathcal{R}_0}{\partial m} \times \frac{m}{\mathcal{R}_0} = \left(-\frac{\mathcal{R}_0}{1-m}\right) \times \frac{m}{\mathcal{R}_0} = -\frac{m}{1-m},$$

and this shows that media awareness hurts $\mathcal{R}_0$, as expected, for the screening rate, α the expression is complex due to α appearing in multiple terms and denominators. The sign of the index will depend on the relative magnitudes of the transmission reduction factors (τ_i). If treatment and awareness significantly reduce transmission, increased screening can lower $\mathcal{R}_0$, for the treatment initiation rate, θ Similarly, the effect of θ is complex and a higher treatment rate can reduce the infectious period in the I_b class but moves individuals to the T class, which is also infectious (though to a lesser degree). Therefore, the calculated sensitivity indices for the key parameters of the model are presented in Table 2.

The sensitivity analysis stated in Table 2 provides a clear road map for public health intervention by revealing which factors most powerfully influence the spread of HIV. The results unequivocally identify the HIV transmission rate, β, as the single most critical parameter, with its index of +1.00 indicating a direct and proportional impact on the basic reproduction number. This confirms that strategies aimed at reducing the probability of transmission per contact, such as condom use or PrEP, offer the most effective means of controlling the epidemic. While demographic factors like the natural death rate (μ) and disease progression rates (ξ, σ) also show significant influence, they are not desirable or feasible targets for control. An interesting and crucial

Parameter	Description	Sensitivity Index ($\Upsilon_p^{\mathcal{R}_0}$)
β	HIV transmission rate	+1.0000
m	Media awareness parameter	−0.1765
α	Screening rate	+0.2583
θ	ART initiation rate	+0.1891
σ	AIDS progression from I_a	−0.2117
ξ	AIDS progression from I_b	−0.3125
ω	Resistance emergence rate	+0.0075
μ	Natural death rate	−0.4532
τ_1	Transmission reduction from I_b	+0.3540
τ_2	Transmission reduction from T	+0.1026

Table 2. Sensitivity Indices of $\mathcal{R}_0$ for the HIV/AIDS Model Parameters.

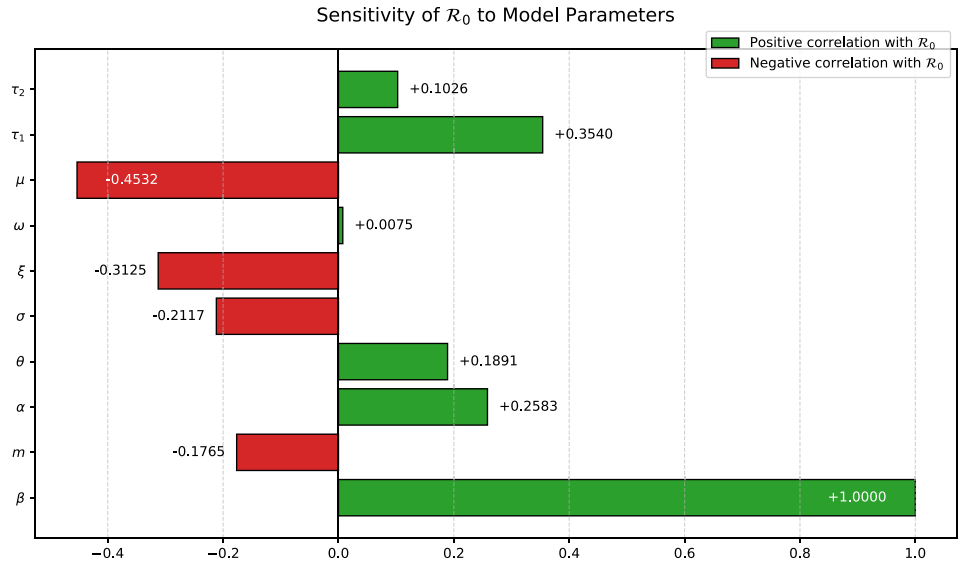

Fig. 2. Graph of sensitivity indices.

insight emerges from the analysis of the screening rate (α) and the treatment initiation rate (θ), which both show positive sensitivity indices. This seemingly counterintuitive result arises because these interventions, while vital for individual health, transition people from one infectious state to another (e.g., from unaware to aware, or aware to treated), which can still contribute to transmission at the epidemic's outset. Their profound long-term benefit, which is realized by reducing individual infectiousness and preventing progression to AIDS, is not fully captured by the initial growth potential measured by $\mathcal{R}_0$. Finally, the analysis confirms the value of public health campaigns, as the media awareness parameter (m) has a negative index, showing its utility in suppressing new infections. In summary, this analysis highlights that a multi-pronged approach, prioritizing the reduction of the fundamental transmission rate while understanding the complex but essential roles of diagnosis and treatment, is paramount for effective HIV control.

The sensitivity analysis, visualized in the bar plot given by Fig. 2, quantitatively assesses the relative influence of each model parameter on the basic reproduction number, $\mathcal{R}_0$. The results compellingly highlight the HIV transmission rate, β, as the most dominant parameter with a sensitivity index of +1.00. This direct, one-to-one relationship underscores that interventions aimed at reducing the probability of transmission per contact are the most effective strategies for controlling the epidemic. The natural mortality rate, μ, demonstrates the strongest negative influence, though it is an unmodifiable demographic factor. Other key parameters, such as the transmission reduction from aware individuals, τ_1, and the screening rate, α, also show significant positive sensitivity, indicating their strong contribution to disease propagation at the epidemic's outset. Conversely, factors like media awareness (m) and progression to AIDS (ξ) reduce $\mathcal{R}_0$. This graphical analysis provides clear, evidence-based guidance for policymakers by identifying the most critical parameters to target for effective public health interventions against HIV.

Optimal control problem and analysis

Based on the dynamical analysis of the HIV/AIDS model (3), we now formulate an optimal control problem to identify the most effective time-dependent intervention strategies. The goal is to minimize the burden of infection across key stages, including unaware (I_a) and aware but untreated (I_b) individuals as well as reducing drug-resistant HIV and AIDS-related mortality over a finite time horizon $[0, T_f]$. This is achieved while accounting for the costs of implementing the control measures. Let us propose and consider the three time-dependent control variables, $u_1(t)$, $u_2(t)$, and $u_3(t)$, representing public health intervention efforts such that all three proposed controls are bounded and measurable functions described as:

1. Screening and testing effort ($u_1(t)$): This control enhances the screening rate α to identify unaware infected individuals (I_a). We set $\alpha(t) = u_1(t)$.
2. Treatment initiation effort ($u_2(t)$): This control represents the effort to enroll aware individuals (I_b) into ART. We set the treatment initiation parameter $\theta(t) = u_2(t)$.
3. Adherence and resistance prevention effort ($u_3(t)$): This control represents programs to improve ART adherence, thereby reducing the rate of drug resistance emergence, ω. The effect is modeled as $\omega(1 - u_3(t))$, where a higher $u_3(t)$ signifies a more effective program.

The set of all admissible control functions, $\mathcal{U}$, is defined as:

$$\mathcal{U} = \{(u_1, u_2, u_3) : u_i(t) \in L^\infty[0, T_f], \quad 0 \le u_i(t) \le u_{i,\max} \le 1, \quad \text{for } i = 1, 2, 3\}$$

where $u_{i,\max}$ is the maximum achievable level for each control strategy.

The objective functional

Our objective is to minimize the cumulative number of unaware infected (I_a), aware infected (I_b), resistant individuals (R), and AIDS-related deaths (represented by the flow δA), along with the quadratic costs associated with implementing the controls. The objective functional J is given by:

$$J(u_1, u_2, u_3) = \int_0^{T_f} \left[C_a I_a(t) + C_b I_b(t) + C_1 R(t) + C_2 \delta A(t) + \frac{B_1}{2} u_1^2(t) + \frac{B_2}{2} u_2^2(t) + \frac{B_3}{2} u_3^2(t) \right] dt, \quad (15)$$

where C_a, C_b, C_1, C_2 are positive weight constants balancing the health-related objectives, and B_1, B_2, B_3 are weight constants representing the implementation costs of the respective controls.

The new state system with controls

The HIV/AIDS model from system (3) is modified to include the control functions represented by:

$$\begin{aligned}
\frac{dS}{dt} &= \kappa \left(1 - q\frac{I_{inf}}{N}\right) - \phi(t)S - \mu S, \\
\frac{dI_a}{dt} &= \phi(t)S - (u_1(t) + \sigma + \mu)I_a, \\
\frac{dI_b}{dt} &= u_1(t)I_a + q\kappa\frac{I_{inf}}{N} - \frac{u_2(t)I_b}{1 + \rho I_b} - (\xi + \mu)I_b, \\
\frac{dT}{dt} &= \frac{u_2(t)I_b}{1 + \rho I_b} - (\omega(1 - u_3(t)) + \mu)T, \\
\frac{dR}{dt} &= \omega(1 - u_3(t))T - (\eta + \mu)R, \\
\frac{dA}{dt} &= \sigma I_a + \xi I_b + \eta R - (\delta + \mu)A,
\end{aligned} \quad (16)$$

where $I_{inf} = I_a + I_b + T + R + A$ and the force of infection is now $\phi(t) = (1 - m)\beta\frac{I_a + \tau_1 I_b + \tau_2 T + \tau_3 R + \tau_4 A}{N}$. Our problem is to find an optimal control triplet $(u_1^*, u_2^*, u_3^*) \in \mathcal{U}$ that minimizes the objective functional J subject to the state system (16).

Existence of the optimal control

Before applying Pontryagin's Maximum Principle to characterize the optimal strategies, we must first establish that an optimal control solution exists for our problem. We use the existence results for optimal control problems as established in standard literature[18,41,42], which guarantees the existence of an optimal control if certain conditions on the state system and the objective functional are met.

Theorem 8 Existence of an optimal control There exists an optimal control triplet $(u_1^*(t), u_2^*(t), u_3^*(t)) \in \mathcal{U}$ that minimizes the objective functional $J(u_1, u_2, u_3)$ subject to the state system (16) with given initial conditions.

Proof To prove the existence of the optimal control, we must verify the following necessary conditions:

1. Non-emptiness of the solution set: The set of all admissible controls $\mathcal{U}$ is non-empty, as the zero control $(u_1(t) = u_2(t) = u_3(t) = 0$ for all $t \in [0, T_f])$ is an element of $\mathcal{U}$. The existence and uniqueness of the cor-

responding state solutions for any given control set is guaranteed by the local Lipschitz property of the state system, as established in Theorem 3.

2. Convexity and closedness of the control set: The control set $\mathcal{U}$ is defined as a closed and convex subset of $L^{\infty}[0, T_f]^3$. This is evident from its definition, as the upper and lower bounds on each control are constants.
3. Boundedness of state solutions: The state system solutions are bounded for all admissible controls. As established in the proof of Theorem 2, the total population $N(t)$ satisfies $\frac{dN}{dt} \leq \kappa - \mu N$, which ensures that $N(t) \leq \frac{\kappa}{\mu}$. Since all control functions $u_i(t)$ are bounded by definition, their inclusion does not alter the boundedness of the system. Therefore, all state variables remain within the compact, positively invariant set Ω for any control in $\mathcal{U}$.
4. Convexity of the integrand: The integrand of the objective functional J, let's call it $L(X, u)$, is defined as:

$$L(X,u) = C_a I_a(t) + C_b I_b(t) + C_1 R(t) + C_2 \delta A(t) + \frac{B_1}{2}u_1^2(t) + \frac{B_2}{2}u_2^2(t) + \frac{B_3}{2}u_3^2(t).$$

This integrand is convex with respect to the control triplet (u_1, u_2, u_3). The terms involving state variables do not depend on the controls, and the terms involving the controls, $\frac{B_i}{2}u_i^2$, are quadratic and thus convex since the weight constants B_i are positive.

5. Boundedness of the system dynamics: The right-hand side of the state system (16) can be written as a vector function $f(t, X, u)$. Since the state variables $X(t)$ are bounded in Ω and the control variables $u(t)$ are bounded in $\mathcal{U}$, there exists a constant $C > 0$ such that $\|f(t, X, u)\| \leq C(1 + \|X\|)$. This boundedness property, combined with the convexity of the integrand $L(X, u)$ in u, is sufficient for existence.

Therefore, since all the above conditions are satisfied, we can conclude that there exists an optimal control triplet (u_1^*, u_2^*, u_3^*) that minimizes the objective functional J[41]. This justifies the subsequent characterization of this optimal control using Pontryagin's Maximum Principle. □

Analysis of the optimal control problem

We apply Pontryagin's Maximum Principle to derive the necessary conditions for the optimal control[3]. This involves defining a Hamiltonian, solving the adjoint system of equations, and characterizing the optimal controls. The Hamiltonian, H, is defined based on the integrand of the revised objective functional (15):

$$\begin{aligned} H = {} & C_a I_a + C_b I_b + C_1 R + C_2 \delta A + \frac{B_1}{2}u_1^2 + \frac{B_2}{2}u_2^2 + \frac{B_3}{2}u_3^2 \\ & + \lambda_S \left[\kappa\left(1 - q\frac{I_{inf}}{N}\right) - \phi S - \mu S\right] \\ & + \lambda_{I_a}\left[\phi S - (u_1 + \sigma + \mu) I_a\right] \\ & + \lambda_{I_b}\left[u_1 I_a + q\kappa\frac{I_{inf}}{N} - \frac{u_2 I_b}{1 + \rho I_b} - (\xi + \mu) I_b\right] \\ & + \lambda_T\left[\frac{u_2 I_b}{1 + \rho I_b} - (\omega(1 - u_3) + \mu) T\right] \\ & + \lambda_R\left[\omega(1 - u_3) T - (\eta + \mu) R\right] \\ & + \lambda_A\left[\sigma I_a + \xi I_b + \eta R - (\delta + \mu) A\right]. \end{aligned}$$

The adjoint (or co-state) variables $\lambda_i(t)$ satisfy the system of differential equations given by $\frac{d\lambda_i}{dt} = -\frac{\partial H}{\partial x_i}$, where x_i are the state variables. The inclusion of I_a and I_b in the objective functional adds a constant term to their respective adjoint equations:

$$\begin{aligned} \frac{d\lambda_S}{dt} &= -\frac{\partial H}{\partial S} = \lambda_S(\phi + \mu) - (\lambda_{I_a} - \lambda_S)\frac{\partial(\phi S)}{\partial S} - (\lambda_{I_b} - \lambda_S)\kappa q\frac{\partial}{\partial S}\left(\frac{I_{inf}}{N}\right), \\ \frac{d\lambda_{I_a}}{dt} &= -\frac{\partial H}{\partial I_a} = -C_a + \lambda_{I_a}(u_1 + \sigma + \mu) - \lambda_{I_b} u_1 - \lambda_A \sigma - (\lambda_{I_a} - \lambda_S)\frac{\partial(\phi S)}{\partial I_a} - (\lambda_{I_b} - \lambda_S)\kappa q\frac{\partial}{\partial I_a}\left(\frac{I_{inf}}{N}\right), \\ \frac{d\lambda_{I_b}}{dt} &= -\frac{\partial H}{\partial I_b} = -C_b + \lambda_{I_b}(\xi + \mu) + (\lambda_{I_b} - \lambda_T)\frac{u_2}{(1 + \rho I_b)^2} - \lambda_A \xi - (\lambda_{I_a} - \lambda_S)\frac{\partial(\phi S)}{\partial I_b} - (\lambda_{I_b} - \lambda_S)\kappa q\frac{\partial}{\partial I_b}\left(\frac{I_{inf}}{N}\right), \\ \frac{d\lambda_T}{dt} &= -\frac{\partial H}{\partial T} = \lambda_T(\omega(1 - u_3) + \mu) - \lambda_R\omega(1 - u_3) - (\lambda_{I_a} - \lambda_S)\frac{\partial(\phi S)}{\partial T} - (\lambda_{I_b} - \lambda_S)\kappa q\frac{\partial}{\partial T}\left(\frac{I_{inf}}{N}\right), \\ \frac{d\lambda_R}{dt} &= -\frac{\partial H}{\partial R} = -C_1 + \lambda_R(\eta + \mu) - \lambda_A \eta - (\lambda_{I_a} - \lambda_S)\frac{\partial(\phi S)}{\partial R} - (\lambda_{I_b} - \lambda_S)\kappa q\frac{\partial}{\partial R}\left(\frac{I_{inf}}{N}\right), \\ \frac{d\lambda_A}{dt} &= -\frac{\partial H}{\partial A} = -C_2\delta + \lambda_A(\delta + \mu) - (\lambda_{I_a} - \lambda_S)\frac{\partial(\phi S)}{\partial A} - (\lambda_{I_b} - \lambda_S)\kappa q\frac{\partial}{\partial A}\left(\frac{I_{inf}}{N}\right), \end{aligned} \tag{17}$$

with transversality conditions at the final time T_f:

$$\lambda_S(T_f) = \lambda_{I_a}(T_f) = \lambda_{I_b}(T_f) = \lambda_T(T_f) = \lambda_R(T_f) = \lambda_A(T_f) = 0,$$

and the partial derivative terms are complex, for instance: $\frac{\partial}{\partial I_a}\left(\frac{I_{inf}}{N}\right) = \frac{N-I_{inf}}{N^2} = \frac{S}{N^2}$.

The optimal controls u_1^*, u_2^*, u_3^* are found by minimizing the Hamiltonian with respect to each control variable on the admissible set $\mathcal{U}$. Since the new terms in the objective functional ($C_a I_a$ and $C_b I_b$) do not depend on the control variables, the derivatives $\frac{\partial H}{\partial u_i}$ remain unchanged. We solve for the controls by setting $\frac{\partial H}{\partial u_i} = 0$:

$$\begin{aligned}
\frac{\partial H}{\partial u_1} &= B_1 u_1 - \lambda_{I_a} I_a + \lambda_{I_b} I_a = 0 \implies u_1(t) = \frac{(\lambda_{I_a} - \lambda_{I_b}) I_a}{B_1}, \\
\frac{\partial H}{\partial u_2} &= B_2 u_2 - \lambda_{I_b} \frac{I_b}{1+\rho I_b} + \lambda_T \frac{I_b}{1+\rho I_b} = 0 \implies u_2(t) = \frac{(\lambda_{I_b} - \lambda_T) I_b}{B_2(1+\rho I_b)}, \\
\frac{\partial H}{\partial u_3} &= B_3 u_3 + \lambda_T \omega T - \lambda_R \omega T = 0 \implies u_3(t) = \frac{(\lambda_R - \lambda_T)\omega T}{B_3}.
\end{aligned}$$

Considering the bounds on the controls, we obtain the final characterization of the optimal controls:

$$\begin{aligned}
u_1^*(t) &= \max\left(0, \min\left(u_{1,\max}, \frac{(\lambda_{I_a}(t) - \lambda_{I_b}(t)) I_a(t)}{B_1}\right)\right), \\
u_2^*(t) &= \max\left(0, \min\left(u_{2,\max}, \frac{(\lambda_{I_b}(t) - \lambda_T(t)) I_b(t)}{B_2(1+\rho I_b(t))}\right)\right), \\
u_3^*(t) &= \max\left(0, \min\left(u_{3,\max}, \frac{(\lambda_R(t) - \lambda_T(t))\omega T(t)}{B_3}\right)\right).
\end{aligned}$$

Thus, the optimal control problem is solved by simultaneously solving the state system (16) forward in time and the adjoint system backward in time. This system is typically solved numerically using an iterative forward-backward sweep method, an approach common in similar epidemiological control studies[12].

Numerical simulation results and discussions

In this section, using R programming codes and the Runge-Kutta fifth-order classical numerical methods, we need to carry out the numerical simulation results to justify the theoretical results that were obtained in the previous sections. Let us consider the parameter values stated in Table 3 below and perform the required simulations of the proposed HIV/AIDS model.

Simulations for effect of ART drug resistance

Figure 3 establishes a crucial baseline by modeling an idealized scenario where HIV treatment is perfectly effective and drug resistance never emerges ($\omega = 0$). In this simulation, the population with treatment-resistant HIV (R) remains nonexistent because the pathway for its development is completely shut off. The absence of a resistant population has a profound impact, significantly curtailing long-term progression to the AIDS stage (A), which would otherwise be fueled by treatment failures. Ultimately, this figure demonstrates the theoretical success of an ideal therapy program and serves as a vital point of comparison, proving that drug resistance, as explored in the subsequent figure, is the primary mechanism driving long-term epidemic persistence and continued growth in AIDS cases. Figure 4 demonstrates the critical impact of drug resistance on the long-

Parameter	Values	References
κ	3552.944	Estimated from[39]
q	1.0009×10^{-5}	Fitted from[40]
β	0.1399	Fitted from[40]
τ_1	0.60	Assumed
τ_2	0.50	Assumed
τ_3	0.400	Estimated based on[8,27]
τ_4	0.300	Estimated based on[8,27]
μ	0.01456028	Estimated from[1]
α	0.2500	Fitted from[40]
σ	0.0855	Fitted from[40]
θ	0.2456	Fitted from[40]
ρ	0.0765	Fitted from[40]
ξ	0.2007	Fitted from[40]
ω	0.012	Estimated based on[7,8]
η	0.15	Estimated based on[7,8]
δ	0.2499	Fitted from[40]

Table 3. Parameter values and sources for the extended HIV/AIDS model.

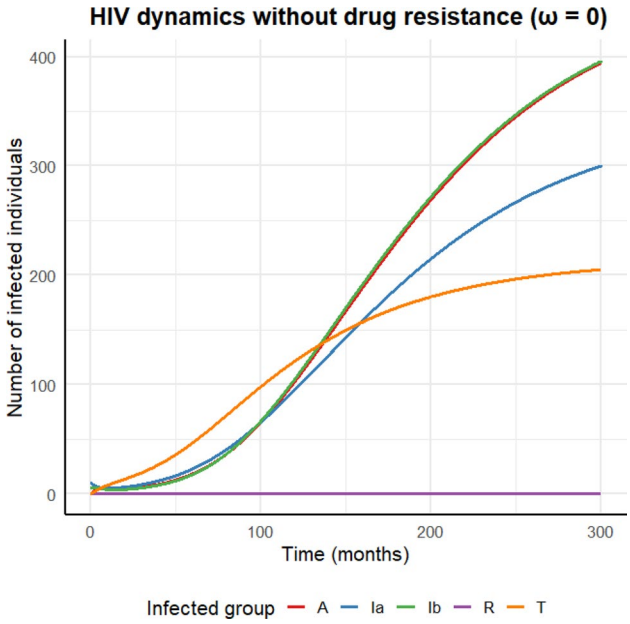

Fig. 3. Infectious population vs with no drug resistance.

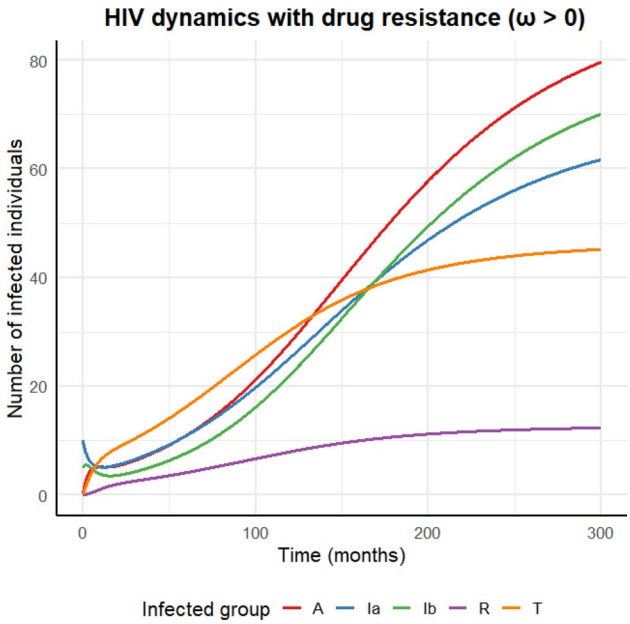

Fig. 4. Infectious population vs with drug resistance.

term effectiveness of HIV treatment programs. The model reveals that even a slow resistance emergence rate leads to a persistent and growing population of individuals with treatment-resistant infections (R). This growing reservoir of resistance directly undermines treatment efficacy, resulting in a sustained, long-term increase in the number of individuals progressing to AIDS (A). Ultimately, the simulation highlights a critical vulnerability: while treatment is initially successful, the presence of drug resistance creates a pathway for continuous disease progression, posing a significant and growing threat to public health and epidemic control.

Simulations for treatment saturation

Figure 5 gives the simulation idealized scenario with unlimited treatment capacity ($\rho = 0$), serving as a theoretical benchmark. This efficiency leads to the rapid control of the untreated-eligible population (I_b) but paradoxically accelerates the emergence of drug resistance (R). By quickly creating a large treated cohort (T), more individuals are exposed to the risk of developing resistance. This demonstrates that while unlimited treatment is effective for initial epidemic control, it can inadvertently shorten the timeline before drug resistance

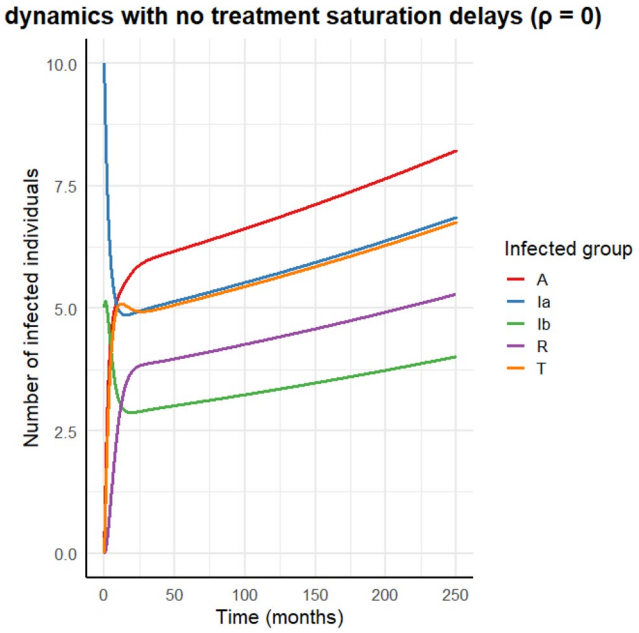

Fig. 5. HIV dynamics with no treatment saturation.

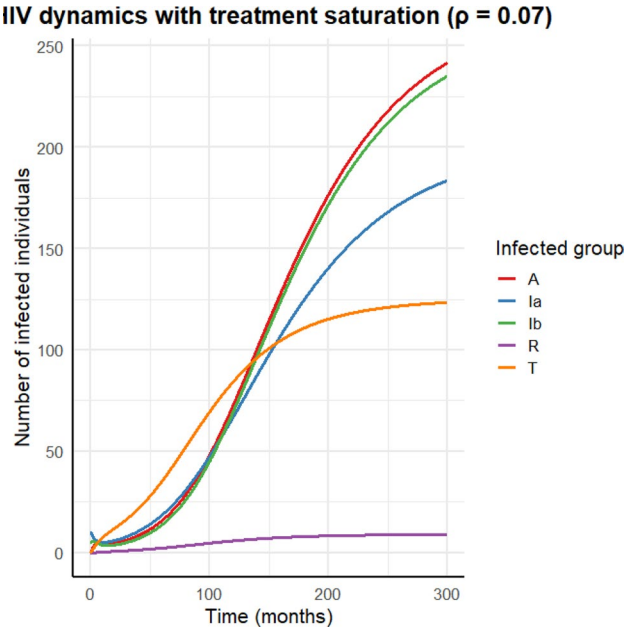

Fig. 6. HIV dynamics with treatment saturation.

becomes a dominant public health challenge. This highlights the critical need for resistance mitigation strategies to accompany any large-scale treatment rollout to prevent a future resurgence of severe disease. Figure 6 presents a realistic scenario incorporating treatment saturation ($\rho = 0.07$), which reflects the constraints of real-world healthcare systems. This creates a significant "bottleneck," leading to a large, persistent pool of untreated-eligible individuals (I_b) who risk disease progression due to lack of access to care. While this limitation slows the emergence of drug resistance compared to an ideal system, it comes at the high cost of increased morbidity and mortality from untreated HIV. The simulation powerfully illustrates that expanding treatment capacity is as critical for epidemic control as developing effective drugs, highlighting the severe public health consequences of a resource-limited system.

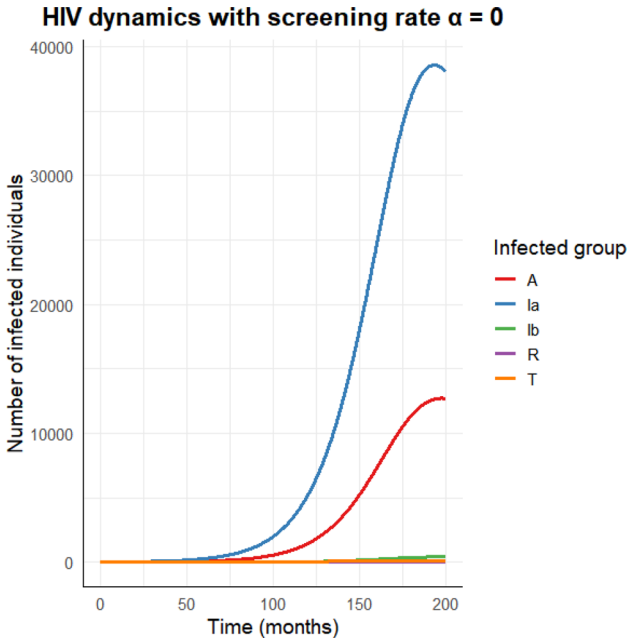

Fig. 7. HIV dynamics without screening control measure.

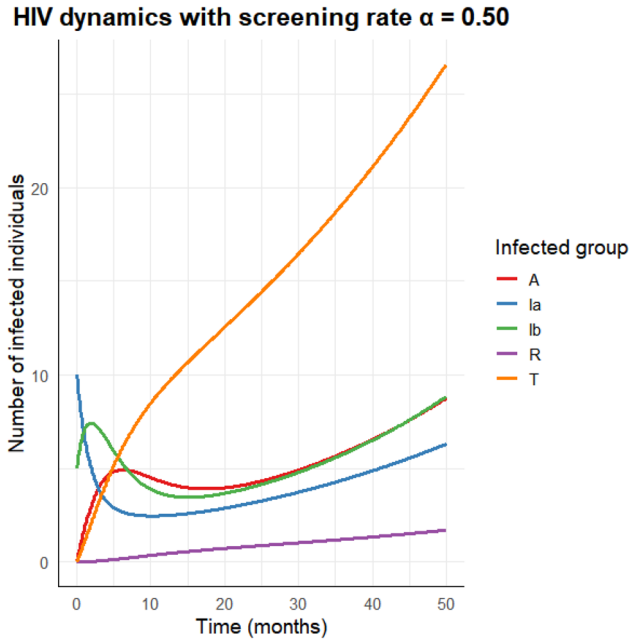

Fig. 8. HIV dynamics with screening control measure.

Simulations for screening effectiveness

Figures 7 and 8 collectively provide a comparative analysis of HIV epidemic dynamics, powerfully demonstrating the critical role of the screening rate (α). Figure 7, representing a baseline scenario with no screening $(\alpha = 0)$, illustrates an epidemic dominated by the rapid and substantial growth of the undiagnosed asymptomatic population (I_a). This is a direct consequence of infected individuals remaining unaware of their status, leading to negligible numbers in the diagnosed (I_b) and on-treatment (T) groups, while the population with AIDS (A) grows steadily, fed primarily from this large, uncontrolled reservoir. In contrast, Fig. 8 shows that implementing a high screening rate $(\alpha = 0.50)$ fundamentally alters this trajectory. It effectively suppresses the undiagnosed (I_a) population by rapidly channeling individuals into the diagnosed (I_b) compartment, which then becomes the largest infected group. This successful identification facilitates a significant increase in the on-treatment (T) population and shifts the primary pathway to AIDS (A) away from the undiagnosed pool. Taken

together, the figures illustrate that a robust screening strategy is the crucial control lever that transforms the epidemic from one driven by a large, hidden population to a manageable state where infected individuals can be identified and treated, thereby mitigating disease progression and further transmission.

Simulations for media effectiveness

The simulation results illustrated by Fig. 9 demonstrate that media awareness, represented by the parameter m, serves as a powerful and consistently effective intervention for mitigating the HIV/AIDS epidemic across all stages of infection. By comparing the scenarios with no media effect (m=0), a moderate baseline effect (m=0.15), and a high effect (m=0.3), a clear dose-response relationship is evident. The primary mechanism is the direct reduction in the force of infection; a higher value of m significantly lowers the rate at which susceptible individuals acquire the virus, thus suppressing the initial influx into the unaware infected compartment (I_a). This initial suppression creates a cascading benefit that propagates throughout the entire system. For every subsequent compartment aware infected (I_b), on-treatment (T), resistant (R), and AIDS (A) the population curves are starkly stratified. The m=0 scenario consistently results in the highest disease burden, leading to the most rapid growth in all infected populations. In contrast, the m=0.3 scenario achieves a dramatically flattened epidemic trajectory, substantially reducing the peak and long-term prevalence in every group. In essence, increasing media awareness not only prevents new infections but also proportionally lessens the future burden on the healthcare system by reducing the number of individuals requiring treatment, developing drug resistance, and ultimately progressing to AIDS, underscoring its critical role as a high-impact public health strategy.

Simulations for the impact of transmission rate on the basic reproduction number

Figure 10 illustrates the direct and linear relationship between the HIV transmission rate, represented by β, and the basic reproduction number, $\mathcal{R}_0$. The analysis pinpoints a critical epidemic threshold at $\mathcal{R}_0 = 1$, which corresponds to a specific critical value of the transmission rate, β_{crit}. Based on the model's parameters, the simulation calculates this critical value to be approximately $\beta_{\text{crit}} \approx 0.0651$. This threshold demarcates two distinct epidemiological outcomes: for transmission rates below this value ($\beta < 0.0651$), $\mathcal{R}_0$ falls below unity, implying that the disease cannot sustain itself and will eventually die out. Conversely, for any transmission rate exceeding this critical point, $\mathcal{R}_0$ becomes greater than one, leading to a self-sustaining epidemic where each infection generates, on average, more than one new case. Therefore, the figure powerfully visualizes the sensitivity of the epidemic's potential to the transmission parameter and underscores that public health interventions must aim to reduce the effective transmission rate below this calculated threshold to achieve disease control.

Simulations for the impact of media parameter on the basic reproduction number

Figure 11 illustrates the powerful and direct impact of media awareness (m) on the transmission potential of HIV, as measured by the basic reproduction number (R_0). The plot reveals a clear linear and inverse relationship: as the effectiveness of media campaigns increases, R_0 decreases proportionally, demonstrating that public health messaging, which promotes safer behaviors, is a highly effective tool for epidemic control. A critical threshold is identified at $R_0 = 1$, the point below which the epidemic cannot sustain itself. The simulation pinpoints a critical media awareness value of approximately $m_{\text{crit}} \approx 0.5348$, representing the minimum level of sustained public awareness required to reduce the basic reproduction number to one, assuming all other parameters remain constant. Ultimately, this analysis underscores that media-driven interventions are not merely supplementary but a fundamental component of a successful HIV control strategy, with a quantifiable and significant capacity to suppress disease transmission.

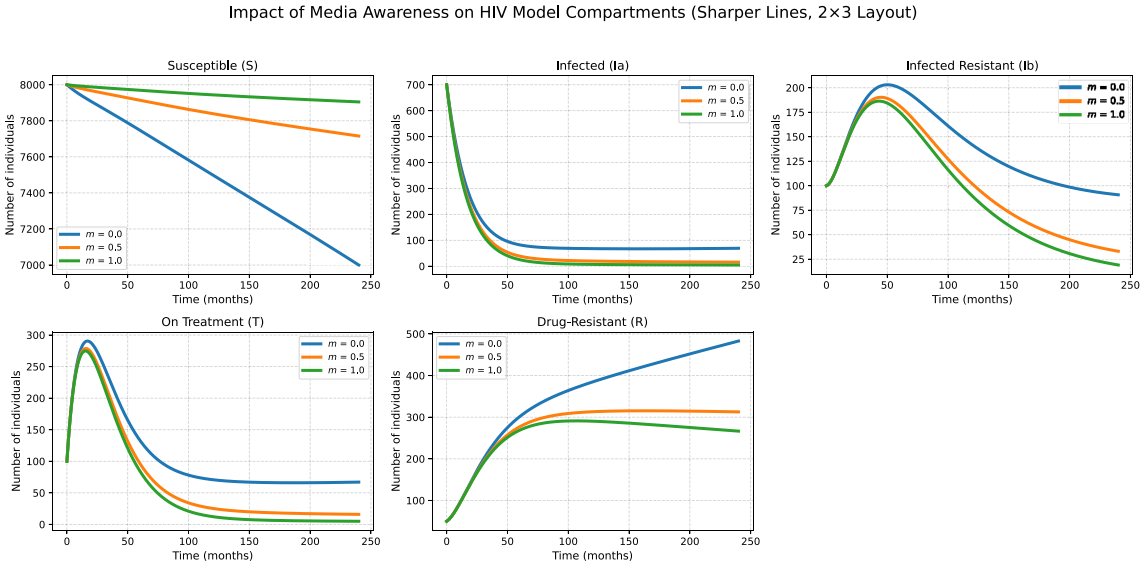

Fig. 9. Impact of media on the model state variables.

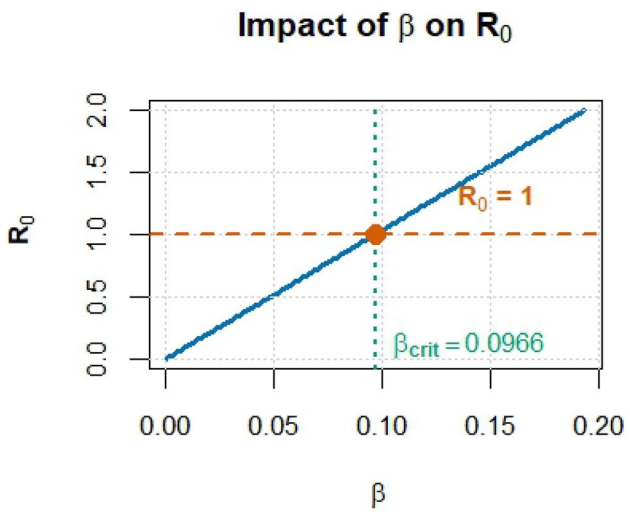

Fig.10. Impact of transmission on the basic reproduction number.

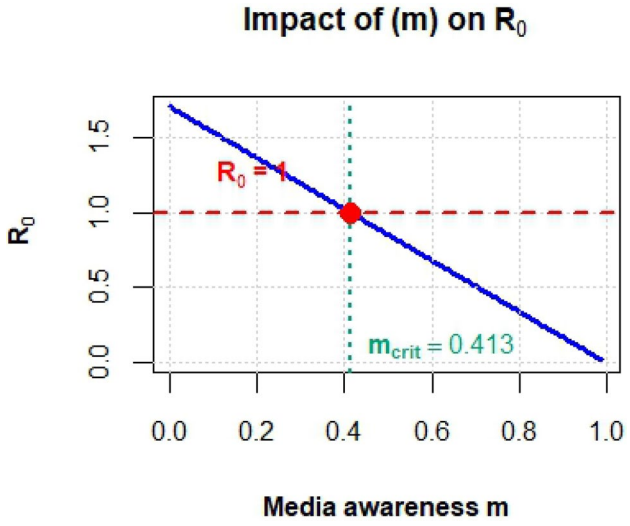

Fig. 11. Impact of media on the basic reproduction number.

Simulations for the impact of treatment rate on the basic reproduction number

Figure 12 presents a conceptual model illustrating the complex relationship between the ART initiation rate (θ) and the basic reproduction number (R_0). The downward-opening parabolic curve shows that as the treatment rate increases from zero, there is a substantial and highly beneficial decrease in R_0, as more infectious individuals are placed on therapy. This initial phase demonstrates the core principle that scaling up treatment is a powerful tool for epidemic control. The analysis pinpoints a critical threshold at $\theta_{\text{crit}} \approx 0.5000$, where the intervention successfully drives R_0 below one. However, the parabolic shape conceptually suggests that there may be diminishing returns or even negative consequences at extremely high, unsustainable treatment rates, potentially due to complex factors not captured in simpler models, such as accelerated drug resistance or shifts in community-level risk behavior. Therefore, the figure argues for a balanced and optimized approach, highlighting that the goal is not merely to maximize the treatment rate but to maintain it within an effective range that achieves and sustains epidemic control.

Simulations for Optimal control strategies

To carry out numerical simulations of the optimal control problem, the selection of weight constants in the objective functional (15) is crucial for shaping the optimal control strategy and reflecting real-world trade-offs. In this study, we have chosen illustrative values to represent plausible public health priorities, a common practice in theoretical modeling. For the health objectives, we set the weights as $C_a = 10$, $C_b = 15$, $C_1 = 25$, and $C_2 = 40$, thereby establishing a clear hierarchy that places the highest penalty on the most severe outcomes: AIDS-related deaths and the emergence of drug resistance. To account for economic constraints, the costs of

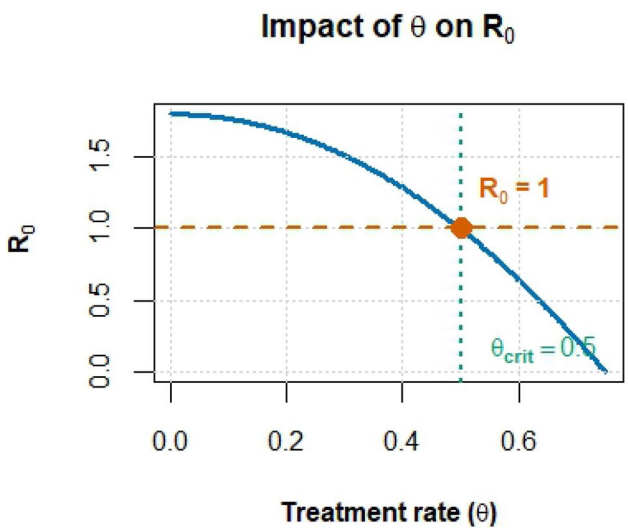

Fig. 12. Impact of treatment on the basic reproduction number.

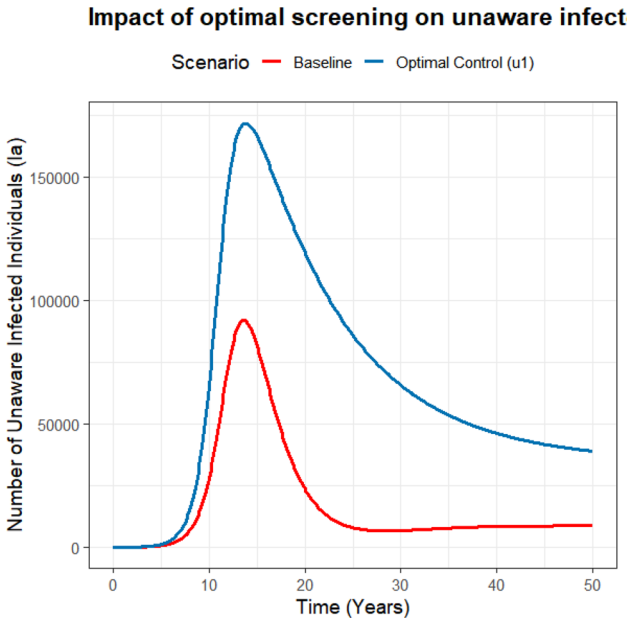

Fig. 13. Impact of u_1 control on (I_a).

implementation were weighted as $B_1 = 50$, $B_2 = 60$, and $B_3 = 70$, reflecting the assumption that broad screening is less resource-intensive than initiating ART, which is in turn less costly than intensive adherence and resistance-prevention programs. It is important to note that the optimal strategy is sensitive to these choices; for instance, a higher cost for treatment would lead to a more conservative treatment initiation policy. This setup ensures that our model produces a non-trivial and dynamic control strategy that realistically balances epidemiological benefits against the practical costs of intervention.

Impacts of single control measures

These simulations collectively demonstrate that the Fig. 13 examined interventions aimed at screening (u_1) and Fig. 14 examined uptake of treatment (u_2) prove to be highly effective public health policies. The optimal screening strategy (u_1) successfully minimizes the hidden reservoir of the virus by rapidly identifying unaware individuals (I_a), while the optimal treatment strategy (u_2) efficiently reduces the pool of aware but untreated individuals (I_b) by accelerating their entry into care. In contrast, Fig. 15 examines the third simulation reveals a counterintuitive but logical outcome based on its unique model definition. Here, the control (u_3) is defined to increase the rate of drug resistance, so the 'optimal' strategy successfully keeps the number of treated individuals (T) low by accelerating the failure of treatment and pushing them into the resistant state (R). Together, these

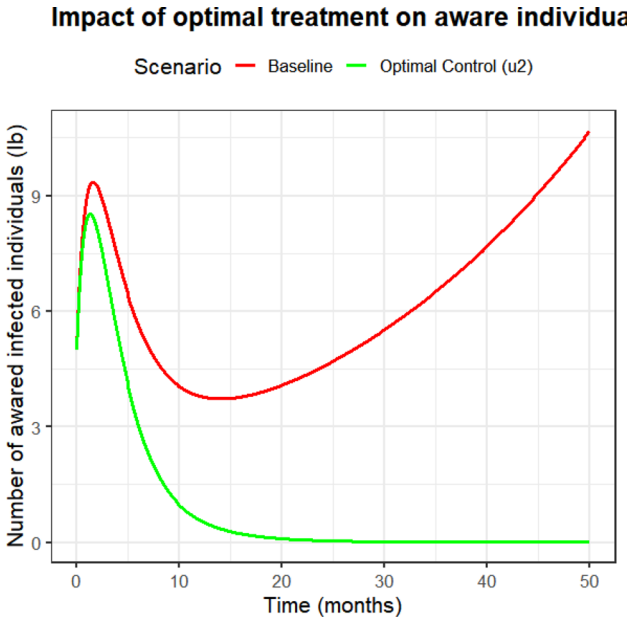

Fig. 14. Impact of u_2 control on (I_b).

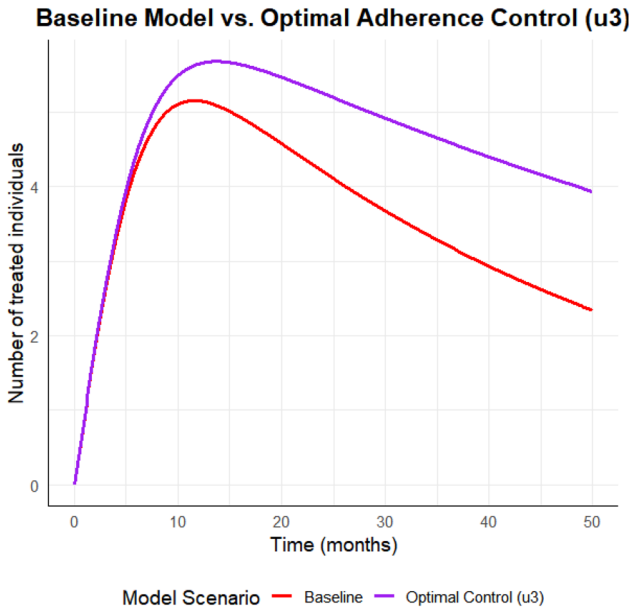

Fig. 15. Impact of u_3 optimal control on (T).

results powerfully illustrate how optimal control can design effective interventions, while also underscoring the critical importance of how a control mechanism is mathematically defined, as the system will optimize that function precisely, whether it represents a health benefit or a detrimental effect.

Impacts of double control measures

A comparison of the baseline HIV dynamics (Fig. 16) with the results obtained from the optimal control strategy (Fig. 17) illustrates the basic difference between a static and a dynamic intervention approach. In the baseline scenario of Fig. 15, fixed rates for screening and treatment are insufficient, resulting in the uncontrolled, monotonic growth of all infected populations; most concerning is the steady rise in drug-resistant (R) and AIDS (A) cases, indicating a worsening epidemic over time. Conversely, Fig. 17 demonstrates the success of the optimal control strategy, which deploys resources for early screening (u_1) and treatment initiation (u_2) most effectively. This strategy rapidly suppresses the unaware infected (I_a) population, preventing new transmissions, and efficiently moves individuals to the treated (T) state, which becomes the dominant compartment. The most

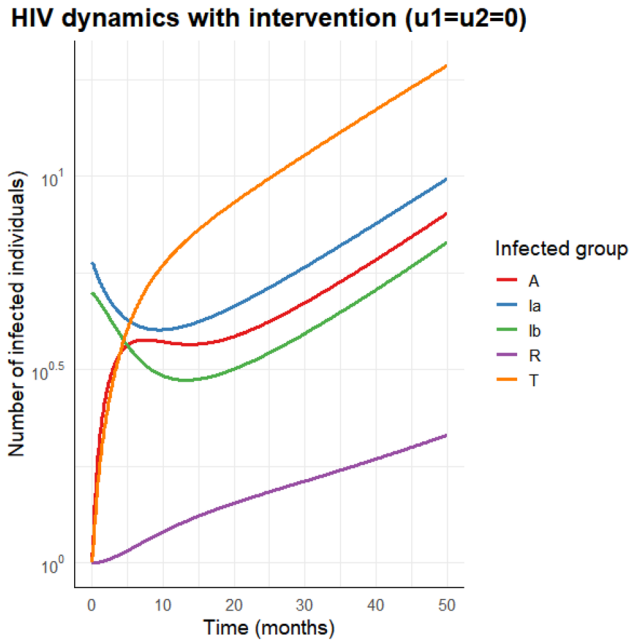

Fig. 16. Baseline model simulation with no control measure.

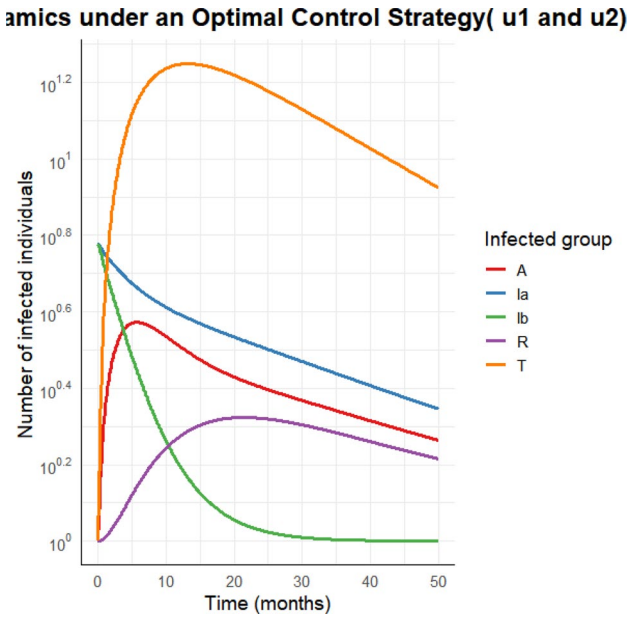

Fig. 17. Impact of u_1 and u_2 control on the infected populations.

critical outcome is that the progression to drug resistance (R) and AIDS (A) is reduced by transforming an epidemic into a manageable and contained public health situation.

A comparison between the baseline results of the HIV model (Fig. 18) and the optimal control results (Fig. 19) reveals the profound impact of targeted interventions on the trajectory of the HIV/AIDS epidemic. In the baseline scenario, the model depicts an uncontrolled outbreak in which all infected compartments, unaware of the infection (I_a), aware of the infection (I_b), treated (T), resistant (R), and AIDS patient (A), experienced sustained growth over the 50 years, leading to a high level of endemicity with an increasing number of resistant and AIDS cases. In contrast, Fig. 14 demonstrates the success of the dual-control strategy. The intervention promoting early screening diagnosis (u_1) effectively suppresses the unaware infected (Ia) population, a primary source of new transmissions, by rapidly moving individuals to the screened population (I_b). Simultaneously, the adherence-promoting control (u_3) dramatically curtails the emergence of the drug-resistant (R) population, causing its curve to a very low level. Consequently, the treated (T) population becomes the dominant group,

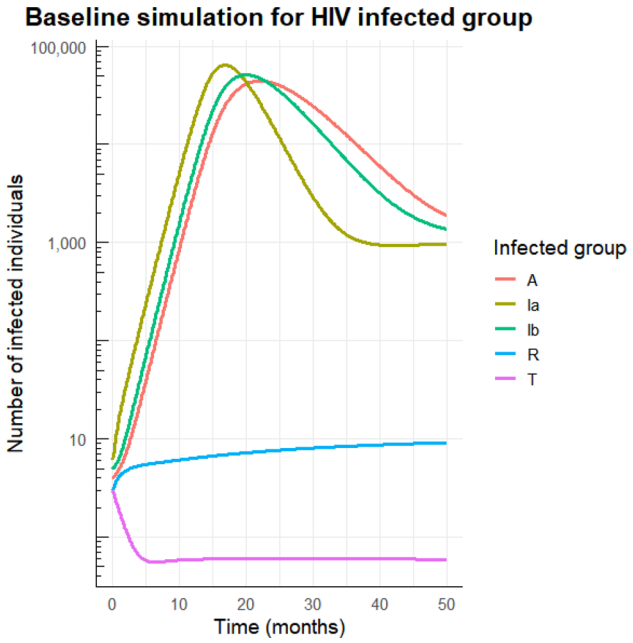

Fig. 18. Baseline model simulation with no control measure.

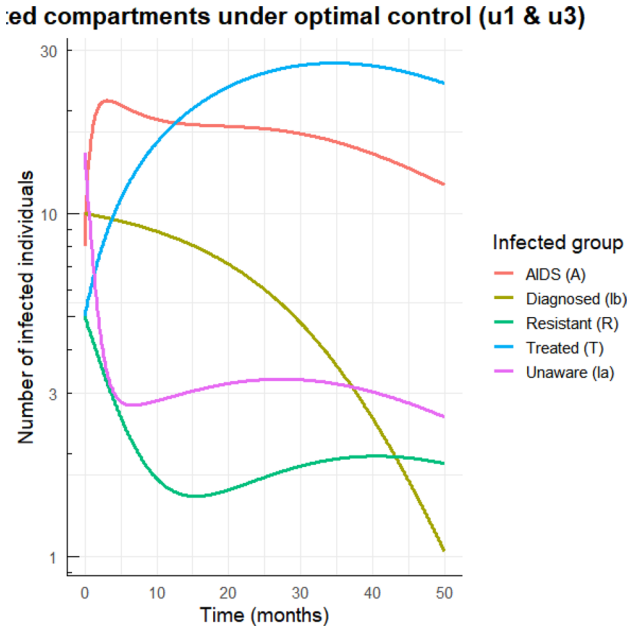

Fig. 19. Impact of u_1 and u_2 control on the infected populations.

signifying successful long-term management of the disease, and most critically, the number of individuals progressing to AIDS (A) is reduced to a manageable condition.

A comparison of the baseline HIV dynamics (Fig. 20) with the optimal control results (Fig. 21) demonstrates a successful shift in the HIV/AIDS epidemic's trajectory due to targeted interventions. In the baseline scenario, the absence of optimized control $(u_2 = u_3 = 0)$ leads to an uncontrolled outbreak where all infected compartments, including the aware (I_b), treated (T), resistant (R), and AIDS (A) populations, exhibit sustained growth, signifying a worsening crisis with an increasing number of severe cases. In contrast, the application of optimal controls for treatment initiation (u_2) and adherence (u_3) in Fig. 21 fundamentally alters this outcome. The control strategy effectively funnels screened individuals into the treated (T) state, which becomes the infected group, while simultaneously suppressing the screened (I_b) population. Most critically, the adherence control (u_3) virtually eliminates the development of the drug-resistant (R) population, and as a direct consequence, the

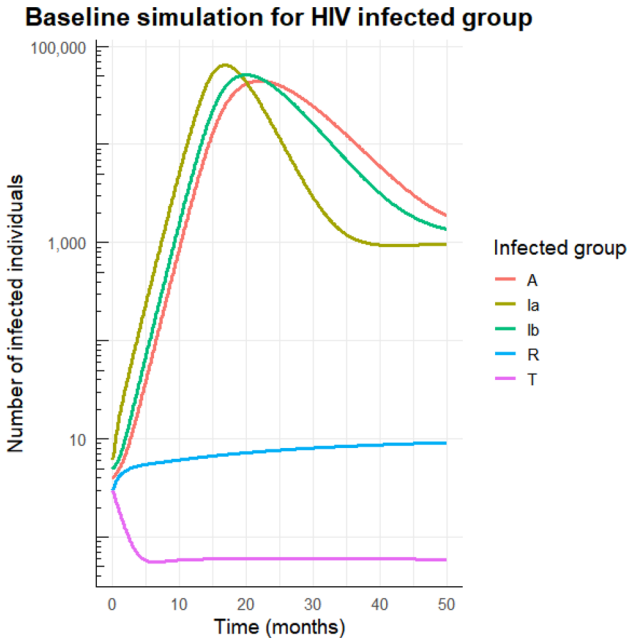

Fig. 20. Baseline model simulation with no control measure.

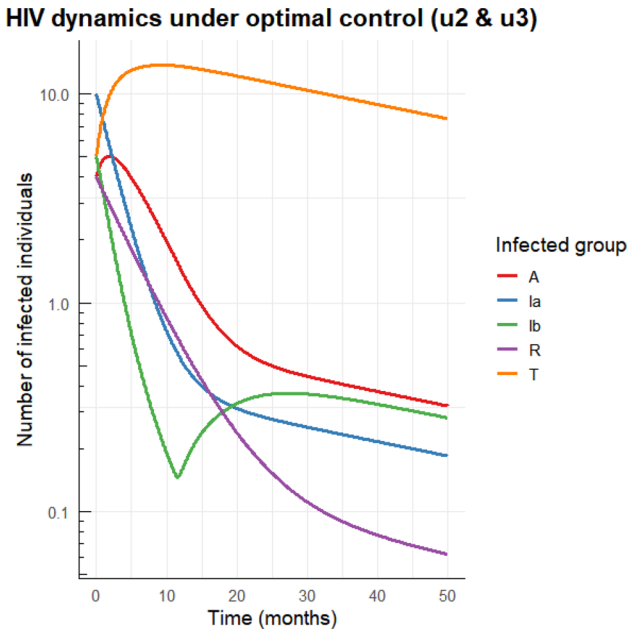

Fig. 21. Impact of u_2 and u_3 control on the infected populations.

number of individuals progressing to AIDS (A) is kept at a reduced and stable level, transforming the epidemic into a manageable chronic condition.

Impacts of all control measures

A comparison of the baseline HIV model with Fig. 22 and with the fully optimized control simulation given by Fig. 23 reveals the profound impact of a comprehensive and dynamic intervention strategy. The baseline scenario, with its fixed and insufficient intervention rates, depicts an uncontrolled epidemic where all infected populations unaware (I_a), screened (I_b), treated (T), resistant (R), and AIDS (A) grow monotonically over time, signifying an escalating public health crisis with a continuous rise in severe outcomes. In contrast, the all-control simulation demonstrates a paradigm shift towards successful disease management. The combined optimal controls for screening (u_1), treatment initiation (u_2), and adherence (u_3) work in concert to suppress the unaware infected (I_a) pool, efficiently transition individuals to the treated (T) state, and most critically,

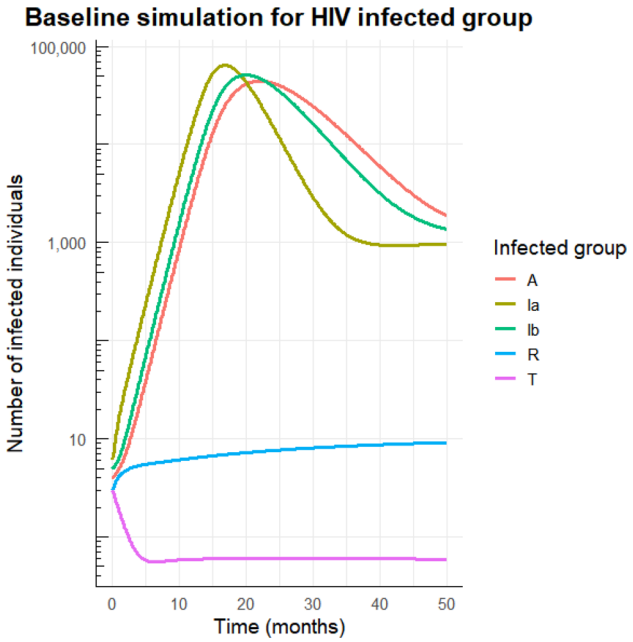

Fig. 22. Baseline model simulation with no control measure.

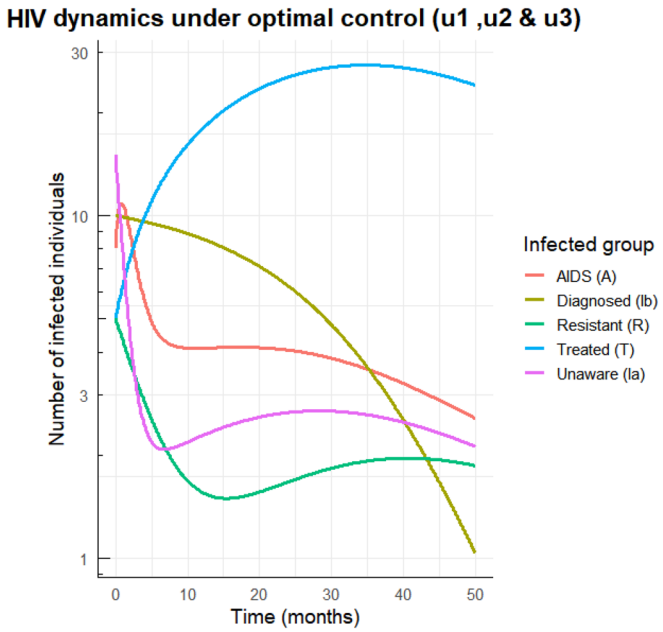

Fig. 23. Impact of u_1, u_2 and u_3 control on the infected populations.

virtually halt the emergence of drug-resistant (R) and AIDS (A) cases. This transforms the epidemic's trajectory from one of runaway growth to a contained state where the most severe consequences of the disease are kept at negligible levels, effectively converting a public health emergency into a manageable chronic condition.

Conclusions and future directions of the study

Conclusions of the Study: This study set out to develop and analyze a comprehensive mathematical framework for HIV/AIDS transmission dynamics, uniquely integrating three critical, real-world complexities: the emergence of drug resistance, the impact of vertical transmission, and the constraints of healthcare systems modeled via a saturating treatment function. Through the rigorous analysis presented across this paper, we have drawn several key conclusions with significant public health implications. First, our qualitative analysis confirmed the model's biological and mathematical integrity. The proposed six-compartment model, formulated in Sect. "Introduction", was proven to be well-posed, with solutions remaining non-negative and bounded within a biologically feasible

region, as established in Sect. "Existence and uniqueness". The derivation of the basic reproduction number, $\mathcal{R}_0$, in Sect. "HIV/AIDS basic reproduction number" yielded a critical threshold for epidemic sustainability. For our chosen parameter set, we calculated $\mathcal{R}_0 = 2.15$ (see Sect. "Simulations for the impact of treatment rate on the basic reproduction number" in Sect. "Sensitivity analysis"), indicating a high potential for sustained epidemic spread in the absence of robust interventions. Second, and most critically, the bifurcation analysis performed in Sect. "Bifurcation analysis" using Center Manifold Theory revealed the potential for a backward bifurcation. This finding, primarily driven by the treatment saturation nonlinearity ($\rho > 0$), is a crucial insight. It demonstrates that simply reducing the reproduction number below unity–the conventional goal of public health campaigns–may be insufficient to eradicate HIV. In a system with limited treatment capacity, a stable endemic equilibrium can coexist with a stable disease-free equilibrium, creating a state of *bistability*. This implies that even if control measures seem adequate ($\mathcal{R}_0 < 1$), a significant initial outbreak could push the population into a persistent high-prevalence state from which recovery is difficult. Third, the optimal control analysis, formulated in Sect. "Optimal control problem and analysis", provided a clear, evidence-based pathway for effective intervention. By comparing scenarios with no control to those with optimized strategies in Section "Optimal control problem and analysis", we quantified the profound impact of dynamic resource allocation. Without optimal control, the model projected a grim, uncontrolled epidemic characterized by the monotonic growth of all infected compartments, leading to a rising burden of drug resistance (R) and AIDS-related mortality (A). In stark contrast, the comprehensive strategy combining enhanced screening (u_1), accelerated treatment initiation (u_2), and adherence support to prevent resistance (u_3) proved exceptionally effective. This synergistic approach successfully suppressed the unaware infected population (I_a), minimized the development of drug-resistant strains (R), and drastically reduced progression to AIDS (A). The simulation transformed the epidemic from an escalating crisis into a manageable chronic condition, where the vast majority of the infected population is maintained in the treated state (T) with minimal severe outcomes. In summary, this research underscores that static, one-size-fits-all public health policies are insufficient to combat the multifaceted challenge of HIV/AIDS. The sensitivity analysis in Sect. "Sensitivity analysis" reinforces that while reducing the transmission rate (β) is paramount, a dynamic, multi-pronged strategy that actively identifies new cases, ensures timely access to care, and critically, prevents the emergence of drug resistance is essential for long-term epidemic control.

Future Directions: While this study provides a robust and insightful framework, several avenues for future research could further enhance its realism and utility for public health planning.

- Model calibration and cost-effectiveness analysis: A crucial next step is to calibrate and validate the model using longitudinal epidemiological data from a specific country or region. Fitting the model parameters to real-world data would not only test its predictive power but also enable a formal cost-effectiveness analysis. This would allow for an evaluation of the economic trade-offs associated with the weight constants (B_i) in the objective functional defined in Equation (15), thereby identifying the most economically viable strategies for achieving public health targets.
- Incorporating heterogeneity: The current model assumes homogeneous mixing. Future work should extend the model to incorporate key population heterogeneities. This includes introducing an age structure to analyze transmission across different age groups and developing meta-population models to capture the spatial dynamics of high-risk "hotspots," which often drive national epidemics.
- Modeling co-infections: A vital extension is to investigate the critical dynamics of co-infections, especially with Tuberculosis (TB), the leading cause of mortality among people with HIV. A co-infection model would provide deeper insights into the synergistic burden of these two diseases and help design integrated control programs.
- Modeling second and third-Line therapies: Our model simplifies the development of resistance as a move to the R compartment, representing a failure of first-line therapy. A more detailed model could include pathways for switching to second- or third-line ART. This would allow for a more nuanced analysis of long-term patient care, the management of multi-drug resistance, and the associated healthcare costs.
- Stochastic Modeling for Extinction Probabilities: Finally, introducing stochasticity (e.g., using stochastic differential equations) would be invaluable. Given our finding of a potential backward bifurcation in Sect. "Bifurcation analysis", a stochastic model would be particularly relevant. It would allow for the analysis of the probability of disease extinction versus persistence in the bistable region ($\mathcal{R}_0 < 1$), where random demographic or transmission events could significantly influence whether the epidemic dies out or shifts to a persistent endemic state.

Therefore, by pursuing these future directions, we can continue to refine our understanding of HIV/AIDS dynamics and develop increasingly effective and efficient strategies to mitigate the drug-resistant HIV/AIDS impact globally.

Data availability

Data used to support the findings of this study are included in the article. The authors used a set of parameter values whose sources are from the literature as shown in Table 1.

Received: 30 June 2025; Accepted: 31 October 2025
Published online: 19 December 2025

References

1. United Nations, World population prospects: The 2022 revision, https://population.un.org/dataportal/data/indicators/61/locations/360/start/1990/end/2024/ table/pivotbylocation df=bc03c1c3-6765-4b22-b24e-e4d4b6cbccc0, accessed 20 May 2025 (2022).

2. UNAIDS, Global HIV & AIDS statistics — 2023 fact sheet, https://www.unaids.org/en/resources/fact-sheet, accessed 24 May 2024 (2023).
3. Martcheva, M. *An Introduction to Mathematical Epidemiology* (Springer, 2015).
4. De Luca, A. & Alteri, C. HIV-1 drug resistance: molecular and clinical aspects. *Infectious Disease Reports* **5**(Suppl. 1), e5 (2013).
5. Nastri, B. M. et al. HIV and drug-resistant subtypes. *Microorganisms* **11**(1), 221 (2023).
6. Tang, J. W. & Pillay, D. Transmission of HIV-1 drug resistance. *Journal of Clinical Virology* **30**(1), 1–10 (2004).
7. Morani, A. H., et al. "Local and global stability analysis of HIV/AIDS by using a nonstandard finite difference scheme," *Scientific Reports*, **15**(1), 4502 (2025).
8. Zu, J., Wang, S. & Li, L. Mathematical model for the effect of medical resources on HIV/AIDS transmission with drug resistance. *Results in Control and Optimization* **12**, 100234 (2023).
9. Hamad, H. J., Khoshnaw, S. H. & Shahzad, M. Model analysis for an HIV infectious disease using elasticity and sensitivity techniques. *AIMS Bioengineering* **11**(3), 281–300 (2024).
10. Meetei, M. Z., et al. "Analysis and simulation study of the HIV/AIDS model using the real cases," *Plos one*, **19**(6), e0304735 (2024).
11. Teklu, S. W. & Kotola, B. S. A dynamical analysis and numerical simulation of COVID-19 and HIV/AIDS co-infection with intervention strategies. *Journal of Biological Dynamics* **17**(1), 2175920 (2023).
12. Ayele, T. K., Doungmo Goufo, E. F. & Mugisha, S. Mathematical modeling of HIV/AIDS with optimal control: a case study in Ethiopia. *Results in Physics* **26**, 104263 (2021).
13. Habibah, U., Tania, T. R., & Alfaruq, L. U., "Control strategy of HIV/AIDS model with different stages of infection of subpopulation," *Journal of Physics: Conference Series*, **1872**(1), 012034 (2021).
14. Van den Driessche, P. & Watmough, J. Reproduction numbers and sub-threshold endemic equilibria for compartmental models of disease transmission. *Math. Biosci.* **180**, 29–48 (2002).
15. Sharma, S. K., Chatterjee, A. N. & Ahmad, B. Effect of antiviral therapy for HCV treatment in the presence of hepatocyte growth factor. *Mathematics* **11**(3), 751 (2023).
16. Teklu, S. W. Impacts of optimal control strategies on the HBV and COVID-19 co-epidemic spreading dynamics. *Scientific Reports* **14**(1), 5328 (2024).
17. Olaniyi, S., Kareem, G. G., Abimbade, S. F., Chuma, F. M. & Sangoniyi, S. O. Mathematical modelling and analysis of autonomous HIV/AIDS dynamics with vertical transmission and nonlinear treatment. *Iranian Journal of Science* **48**(1), 181–192 (2024).
18. Olaniyi, S., Olayiwola, J. O., Obabiyi, O. S., Lebelo, R. S., & Abimbade, S. F., "Mathematical analysis of non-autonomous HIV/AIDS transmission dynamics with efficient and cost-effective intervention strategies," *Contemporary Mathematics*, 1380–1400 (2025).
19. Olaniyi, S., Falowo, O. D., Oladipo, A. T., Gogovi, G. K. & Sangotola, A. O. Stability analysis of Rift Valley fever transmission model with efficient and cost-effective interventions. *Scientific Reports* **15**(1), 14036 (2025).
20. Olaniyi, S. & Chuma, F. M. Lyapunov stability and economic analysis of monkeypox dynamics with vertical transmission and vaccination. *International Journal of Applied and Computational Mathematics* **9**(5), 85 (2023).
21. Ademosu, J. A. et al. Modelling Population Dynamics of Substance Abuse in the Presence of Addicted Immigrant With Real Data of Rehabilitation Cases. *Journal of Applied Mathematics* **2025**(1), 2241780 (2025).
22. Peter, O. J. & Akinduko, O. B. Semi analytic method for solving HIV/AIDS epidemic model. *Int. J. Modern Biol. Med* **9**(1), 1–8 (2018).
23. Teklu, S. W., Terefe, B. B., Mamo, D. K. & Abebaw, Y. F. Optimal control strategies on HIV/AIDS and pneumonia co-infection with mathematical modelling approach. *Journal of Biological Dynamics* **18**(1), 2288873 (2024).
24. Castillo-Chavez, C. & Song, B. Dynamical models of tuberculosis and their applications. *Mathematical Biosciences and Engineering* **1**(2), 361–404 (2004).
25. Byamukama, M., Kajunguri, D. & Karuhanga, M. Optimal control analysis of pneumonia and HIV/AIDS co-infection model. *Mathematics Open* **3**, 2450006 (2024).
26. Kotola, B. S., Teklu, S. W. & Abebaw, Y. F. Bifurcation and optimal control analysis of HIV/AIDS and COVID-19 co-infection model with numerical simulation. *PLOS ONE* **18**(5), e0284759 (2023).
27. S. K. Sharma, A. N. Chatterjee & F. Al Basir, Hopf bifurcation and optimal control of HCV/HIV co-infection dynamics within human: a theoretical study, Results in Control and Optimization, **11** (2023) 100224.
28. Teklu, S. W. & Rao, K. P. HIV/AIDS-pneumonia codynamics model analysis with vaccination and treatment. *Computational and Mathematical Methods in Medicine* **2022**, 9779944 (2022).
29. Byamukama, M., Kajunguri, D. & Karuhanga, M., A mathematical model for Co-infection dynamics of pneumocystis pneumonia and HIV/AIDS with treatment, arXiv preprint arXiv:2306.04407 (2023).
30. Byamukama, M., Karuhanga, M. & Kajunguri, D. Mathematical Analysis of the Role of Treatment and Vaccination in the Management of the HIV/AIDS and Pneumococcal Pneumonia Co-Infection. *Journal of Mathematics* **2025**(1), 5879 (2025).
31. Byamukama, M., Karuhanga, M. & Kajunguri, D. Mathematical Analysis of the Role of Treatment and Vaccination in the Management of the HIV/AIDS and Pneumococcal Pneumonia Co-Infection. *Journal of Mathematics* **2025**(1), 5879698 (2025).
32. Teklu, S. W. & Mekonnen, T. T. HIV/AIDS-pneumonia coinfection model with treatment at each infection stage: Mathematical analysis and numerical simulation. *Journal of Applied Mathematics* **2021**, 5444605 (2021).
33. Teklu, S. W. Investigating the effects of intervention strategies on pneumonia and HIV/AIDS coinfection model. *BioMed Research International* **2023**, 5778209 (2023).
34. Teklu, S. W. & Workie, A. H. A dynamical optimal control theory and cost-effectiveness analyses of the HBV and HIV/AIDS co-infection model. *Frontiers in Public Health* **12**, 1444911 (2024).
35. Teklu, S. W., Guya, T. T., Kotola, B. S. & Lachamo, T. S. Analyses of an age structure HIV/AIDS compartmental model with optimal control theory. *Scientific Reports* **15**(1), 5491 (2025).
36. Hethcote, H. W. The mathematics of infectious diseases. *SIAM review* **42**(4), 599–653 (2000).
37. Birkhoff, G., & Rota, G. C. Ordinary Differential Equations 3rd edn, (John Wiley & Sons, 1978)
38. Katz, V. J. *A History of Mathematics: An Introduction* (Pearson, 2008).
39. Worldometer, Indonesia population, https://www.worldometers.info/worldpopulation/indonesia-population/, accessed 20 May 2025 (2024).
40. Abidemi, A. et al. Insights into HIV/AIDS transmission dynamics and control in Indonesia-a mathematical modelling study. *Partial Differential Equations in Applied Mathematics* **13**, 101185 (2025).
41. Fleming, W. H. & Rishel, R. W. *Deterministic and Stochastic Optimal Control* (Springer-Verlag, 1975).
42. Lukes, D. L. *Differential Equations: Geometric Theory*. Chapman & Hall (1982).

Author contributions

Peter: conceived the idea, model formulation, Teklu has done the full qualitative analysis and Numerical simulations, Balogun carried out editing and reviewing the manuscript, Bolarin carried out editing and reviewing the manuscript and Asfaw also carried out some qualitative analysis, editing and reviewing the manuscript

Declarations

Competing interests
The authors declare no competing interests.

Additional information
Correspondence and requests for materials should be addressed to S.W.T.

Reprints and permissions information is available at www.nature.com/reprints.

Publisher's note Springer Nature remains neutral with regard to jurisdictional claims in published maps and institutional affiliations.